

INCREASING THE EFFICIENCY OF CAM FOLLOWER SYSTEMS  
THROUGH ENERGY RECOVERY

by

William Oishi

A thesis submitted to the  
School of Graduate and Postdoctoral Studies in partial  
fulfillment of the requirements for the degree of

Masters of Applied Science in Mechanical Engineering

The Faculty of Engineering and Applied Science

University of Ontario Institute of Technology

Oshawa, Ontario, Canada

August 2019

© William Oishi, 2019

# Thesis Examination Information

## Master of Applied Science in Mechanical Engineering

Thesis title: Increasing the Efficiency of Cam Follower Systems Through Energy Recovery

An oral defense of this thesis took place on August 7, 2019 in front of the following examining committee:

### Examining Committee:

Chair of Examining Committee	Dr. Carlos Rossa
Research Supervisor	Dr. Brendan MacDonald
Examining Committee Member	Dr. Dipal Patel
External Examiner	Dr. Sayyed Ali Hosseini, UOIT Manufacturing Engineering Faculty

The above committee determined that the thesis is acceptable in form and content and that a satisfactory knowledge of the field covered by the thesis was demonstrated by the candidate during an oral examination. A signed copy of the Certificate of Approval is available from the School of Graduate and Postdoctoral Studies.

# Abstract

A cam and follower system is a mechanical linkage designed to transform a rotating motion to that of a linear reciprocating motion. Cams are well known for valving in internal combustion engines but are commonly utilized in industrial processes including stamping, food processing, and textile manufacturing. Most systems use an input torque in order to produce a linear force during the rise portion and rely on a spring to produce the return motion on the fall. Experiments using multiple test apparatuses suggest that the commonly used 30 degree pressure angle limit can be exceeded in low speed applications. Results also show that energy can be recovered from the system during the fall portion when the follower subjects the cam to a high return force. An analytical analysis describes the characteristics of how this return force can be recovered to increase overall system efficiency.

**Keywords:** Cam Follower; Pressure Angle; Energy Recovery

## Author's Declaration

I hereby declare that this thesis consists of original work of which I have authored. This is a true copy of the thesis, including any required final revisions, as accepted by my examiners.

I authorize the University of Ontario Institute of Technology to lend this thesis to other institutions or individuals for the purpose of scholarly research. I further authorize University of Ontario Institute of Technology to reproduce this thesis by photocopying or by other means, in total or in part, at the request of other institutions or individuals for the purpose of scholarly research. I understand that my thesis will be made electronically available to the public.

William Oishi

---

# Acknowledgements

I would first like to thank my supervisor, Dr. Brendan MacDonald, for without his guidance and continued inspiration I would not have had this opportunity. Your persistence and passion to understand the why and how of everything around you is something I will always admire.

To the colleagues I now call close friends in the MacDonald Lab: Anders Nielsen, Salvatore Ranieri, Justin Rizzi, Henry Fung, Michael Crowley, Md. Almostasim Mahmud, and Brayden York, I cannot thank you enough for the support and inspiration you've provided over these past years. The late nights, frustrating results, and never ending deadlines may eventually fade from memory but the passionate debates, celebratory successes, and life lessons will never be forgotten. A special thanks and Henry and Justin for their guidance and support while learning and developing a functional understanding of both Python and Arduino which proved to invaluable. To my sister Vanessa for her late night help with my figures.

Many thanks to my examiners Dr. Dipal Patel, Dr. Sayyed Ali Hosseini, and Dr. Brendan MacDonald for both agreeing to evaluate my work and taking the time to be part of my examining committee.

Lastly to my parents Ellis and Nancy Oishi, for their never ending support. Without both of you I would not be where I am today and I cannot thank you enough. Your inspiration and drive have encouraged me to work hard in all aspects of my life and I will be forever grateful.

## Statement of Contributions

The following piece was the sole responsibility of the author. Standard referencing has been used to acknowledge any ideas or materials that belong to others. As of the submission date, none of the work contained within this thesis has been submitted for publication.

# Contents

<b>Abstract</b>	<b>iii</b>
<b>Author's Declaration</b>	<b>iv</b>
<b>Acknowledgements</b>	<b>v</b>
<b>Statement Of Contributions</b>	<b>vi</b>
<b>List of Tables</b>	<b>ix</b>
<b>List of Figures</b>	<b>ix</b>
<b>Nomenclature</b>	<b>xi</b>
<b>1 Introduction</b>	<b>1</b>
1.1 Background . . . . .	3
1.1.1 Cam Design Considerations . . . . .	3
1.1.2 Pressure Angle . . . . .	3
1.1.3 Cam Profile Displacement Programs . . . . .	5
1.1.4 Torque . . . . .	9
1.2 Literature Review . . . . .	12
1.2.1 Cam Synthesis . . . . .	12
1.2.2 Selecting Cam Parameters . . . . .	15
1.2.3 Design Limitation . . . . .	16
Pressure Angle Limitations . . . . .	17
1.2.4 Cam Phenomenon . . . . .	18
1.3 Gaps in Current Literature . . . . .	18
1.4 Thesis Objectives . . . . .	20
<b>2 Experimental Apparatus and Methods</b>	<b>21</b>
2.1 Apparatus Overview . . . . .	22
2.1.1 Dynamic Test Apparatus . . . . .	22
2.1.2 Static Test Apparatus . . . . .	25
2.2 Uncertainty and Sources of Error . . . . .	29
2.2.1 Dynamic Cam Tester Error . . . . .	29
2.2.2 Static Cam Tester . . . . .	30
2.2.3 Round Profile Test . . . . .	31

2.3	Experimental Method . . . . .	33
2.3.1	Dynamic Cam Tester Procedure . . . . .	33
2.3.2	Static Cam Tester Fixed Position Procedure . . . . .	33
2.3.3	Static Cam Tester Variable Position Procedure . . . . .	34
<b>3</b>	<b>Results and Discussion</b>	<b>35</b>
3.1	Comparison of Torque Forces . . . . .	35
3.2	Pressure Angle Limitations . . . . .	41
3.3	Dynamic Tests . . . . .	43
3.3.1	Acrylic Cam Profile Testing . . . . .	43
3.3.2	Constant Pressure Angle Testing . . . . .	45
3.4	Static Tests . . . . .	47
3.4.1	Static Testing (no spring) . . . . .	47
3.5	Conclusion . . . . .	50
3.5.1	Recommendations . . . . .	51
	<b>Bibliography</b>	<b>52</b>



# List of Tables

# List of Figures

Figure 1.1	Cam nomenclature . . . . .	4
Figure 1.2	Basic cycloidal motion curves of displacement, velocity, acceleration, and jerk . . . . .	6
Figure 1.3	Basic 3-4-5 polynomial motion curves of displacement, velocity, acceleration, and jerk . . . . .	8
Figure 1.4	Comparison of common displacement programs considering follower rise $h$ and duration $\beta$ . . . . .	9
Figure 1.5	Free body diagram of a high speed cam . . . . .	10
Figure 2.1	a) Photo of dynamic test apparatus b) Schematic of Experimental Setup: 1)pneumatic cylinder, 2)load cell, 3)Arduino, 4)laptop, 5)power supply, 6)NEMA 19 stepper motor, 7)NEMA 23 stepper motor and gearbox, 8) follower, 9)cam profile, 10)adjustable offset base, 11)pressure regulator, 12)pressure transducer . . . . .	24
Figure 2.2	A) Photo of static test apparatus with fixed cam b) Static force tester schematic with fixed cam placement: 1) linear actuator, 2) load cell, 3) follower, 4) cam, 5) laptop, 6) Arduino, 7) power supply 8) adjustable stop . . . . .	27
Figure 2.3	a) Photo of static force tester with variable cam angle and sprung moment arm b) Static force tester schematic with fixed cam placement: 1) linear actuator, 2) load cell, 3) cam profile, 4) follower, 5)laptop, 6) Arduino, 7) power supply 8) adjustable stop, 9) spring . . . . .	28
Figure 2.4	Distribution of forces as a percentage of the applied load on a circular cam profile . . . . .	32
Figure 3.1	Comparison of forces when comparing torque applied to a cam and torque imparted on a cam by the follower . . . . .	38

Figure 3.2	Input and output torque as a function of pressure angle including the respective ratio of output torque to input torque .	40
Figure 3.3	Input torque relative to pressure angle assuming unit radius $r$ and unit force $F_a$ . . . . .	41
Figure 3.4	Axial and lateral components of applied force based on pressure angle . . . . .	43
Figure 3.5	Comparison of lateral forces on steel and plastic cam profiles	44
Figure 3.6	Polynomial steel and acrylic cam profiles: 30, 30, 25, and 20 degrees from top left to bottom right) . . . . .	45
Figure 3.7	Lateral load produced by 30, 35 and 40 degree pressure angle cams . . . . .	46
Figure 3.8	From top to bottom 20, 30, 35, and 40 degree constant pressure angle cam profiles . . . . .	47
Figure 3.9	Constant pressure angle cam profiles . . . . .	48
Figure 3.10	. . . . .	49

# Nomenclature

$\alpha$	Pressure Angle	degrees
$\beta$	Cam Cycle Duration(Rise, Fall, Dwell)	degrees
$\omega$	Angular Velocity	$\frac{rad}{s}$
$\theta$	Cam Angle	degrees
$F_a$	Force applied axially through or by the follower	N
$F_l$	Force applied laterally through or by the follower	N
$F_n$	Normal Force	N
$h$	Maximum Follower Rise	m
$N$	Normal Component of Velocity	$\frac{m}{s}$
$r$	Distance From Cam Center to Follower Center	m
$r_b$	Base Circle Radius	m
$R_p$	Prime Circle Radius	m
$T$	Torque	Nm

# Chapter 1

## Introduction

As climate change becomes an ever growing issue, the importance of becoming less reliant on fossil fuels and increasing the efficiency of current and future systems is becoming more evident. While modern technology is constantly advancing and evolving, there are many instances in which the reevaluation of older technologies have given rise to advancements in modern designs. Even though mechatronics has led to a drastic increase in the use of microelectronics and various electric motors in attempt to replace mechanical linkages, there are many situations in which the cost and efficiency do not result in an overall benefit. When sinusoidal motion is not desirable but a repeatable movement with a specific motion is required, a cam-follower system is often a good solution.

Traditional cam applications such as controlling valves in an engine, driving the motion of a sewing machine, or various processes in industrial manufacturing, they are often limited to a range of forces. A major consideration regarding cam-follower systems is that they demand an electrical or mechanical input, thus, the torque

required to rotate the cam is a necessary input. This results in it continually acting as a parasitic loss on the system.

In order to develop an efficient cam follower system, various constraints around the design parameters are selected such as the cam size, profile, follower travel length, offset, and pressure angle. By fixing one or more of these parameters due to physical restrictions or best practices, an efficient cam profile can be generated to minimize the amount of energy it consumes. Physical constraints are often dictated by the application but the suggested limitations of pressure angle are unclear. Traditional cams are used in applications where they consume power, thus acting as a parasitic loss while converting rotational motion into that of an axial or pivoting motion. In order to design effective cam follower systems with higher efficiency, not only do pressure angle limitations have to be better understood, but the ability of the system to potentially recover energy needs to be considered. This thesis aims to further investigate the potential of energy recovery and how it relates to the energy input to the system, as well as the effects of pressure angle and the widely accepted 30 degree pressure angle limit for radial cams with roller followers.

## 1.1 Background

### 1.1.1 Cam Design Considerations

The cam follower system appears simple by inspection but is surprisingly complex in both the creation of its geometry and the method by which it is designed. When the cam geometry is being designed, the displacement, velocity, acceleration, and jerk all need to be taken into consideration in order to operate smoothly, especially when considering high speed applications [1–3]. While the follower plays a roll in the limitation of the cam’s motion, this study looks solely at the roller type follower as it provides many advantages over other common follower shapes such as the flat faced or knife edge follower. When designing the cam profile, simple harmonic, cycloidal, and polynomial cam designs all provide various advantages in design simplicity, ease of fabrication, and operating characteristics. In attempts to optimize the design of a cam-follower system, the complexity arises from the number of variables that need to be considered. The size of the follower, base circle, pitch profile, direction of rotation, offset, pressure angle limit, required torque, follower displacement, and rotational velocity all play a key part in its successful operation [1,2,4].

### 1.1.2 Pressure Angle

Of the many design considerations, pressure angle has been determined to be one of the most important when creating a cam-follower system [1,2,4,5]. It is described as the angle between the axis of transmission and the followers direction of motion. The axis of transmission as shown in Figure 1.1, can be described as the axis normal

to the tangent of the curve between the follower and cam profile. This is important as the pressure angle determines which portion of the force transmitted by the cam to the follower is useful.

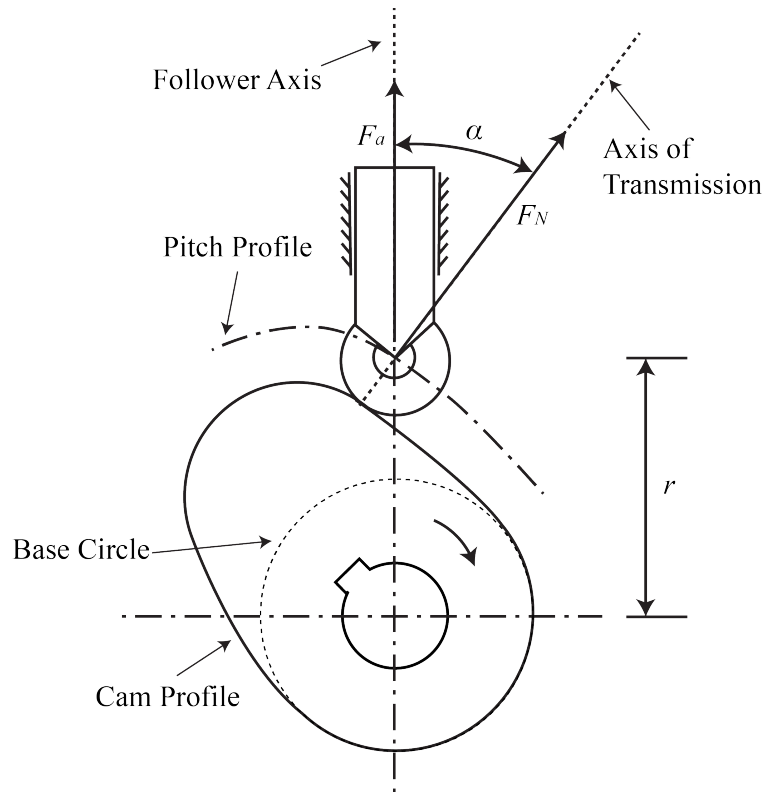


**Figure 1.1:** Cam nomenclature

As the pressure angle is increased from 0 degrees (completely axial force through the follower) towards the suggested limit of 30 degrees, the amount of lateral force being applied to the follower will reach 50 percent of the total applied force.

As seen in Figure 1.1, the lateral and axial force components of the total force are a function of the sine and cosine functions of a given pressure angle  $\alpha$ . The lateral force increases the friction seen by the follower guides as well as the resulting bending moment applied to the follower. This can result in excessive wear which may lead to premature failure of the follower [6].

### 1.1.3 Cam Profile Displacement Programs

Cam follower systems are often chosen because of their ability to produce a non-sinusoidal motion with a sinusoidal input with the ability to dwell. This ability to dwell, while also controlling the velocity, and acceleration profiles is extremely important in many mechanical processes. While this is something that can often be replaced by a stepper or servo motor, a cam-follower is reliable and is often able to be operated off of the existing motion of the machine which can be more effective.

When designing the profile, the duration of the required dwells and required displacements must be known. Once these are determined, it is possible to generate the cam profile that the follower will travel along [7]. The dynamics of a cam profile are ultimately a function of the type of displacement program that is chosen. Uniform motion, parabolic motion, simple harmonic motion, cycloidal, and polynomial profiles all offer different dynamic characteristics. Uniform motion will result in infinite acceleration, similarly parabolic motion and simple harmonic motion both result in infinite jerk. Achieving a profile with finite jerk, is important for obtaining a cam profile with reduced wear characteristics [1, 2, 4, 7].

When high speed operation is desired, cycloidal displacement programs are often used as they offer finite jerk at the beginning and end of the transitions between dwells. The displacement, velocity, acceleration, and jerk profiles can be easily represented as a function of cam angle but the maximum pressure angle must still be taken into consideration. Using the equations below, a basic cycloidal cam profile can be generated assuming a duration  $\beta$  and rise  $h$  have been established.



Cycloidal Cam Profile [2]:

$$\text{Displacement} \quad y = h \left( \frac{\theta}{\beta} - \frac{1}{2\pi} \sin \frac{2\pi\theta}{\beta} \right) \quad (1.1)$$

$$\text{Velocity} \quad y' = \frac{h}{\beta} \left( 1 - \cos \frac{2\pi\theta}{\beta} \right) \quad (1.2)$$

$$\text{Acceleration} \quad y'' = \frac{2h\pi}{\beta^2} \sin \frac{2\pi\theta}{\beta} \quad (1.3)$$

$$\text{Jerk} \quad y''' = \frac{4h\pi^2}{\beta^3} \cos \frac{2\pi\theta}{\beta} \quad (1.4)$$

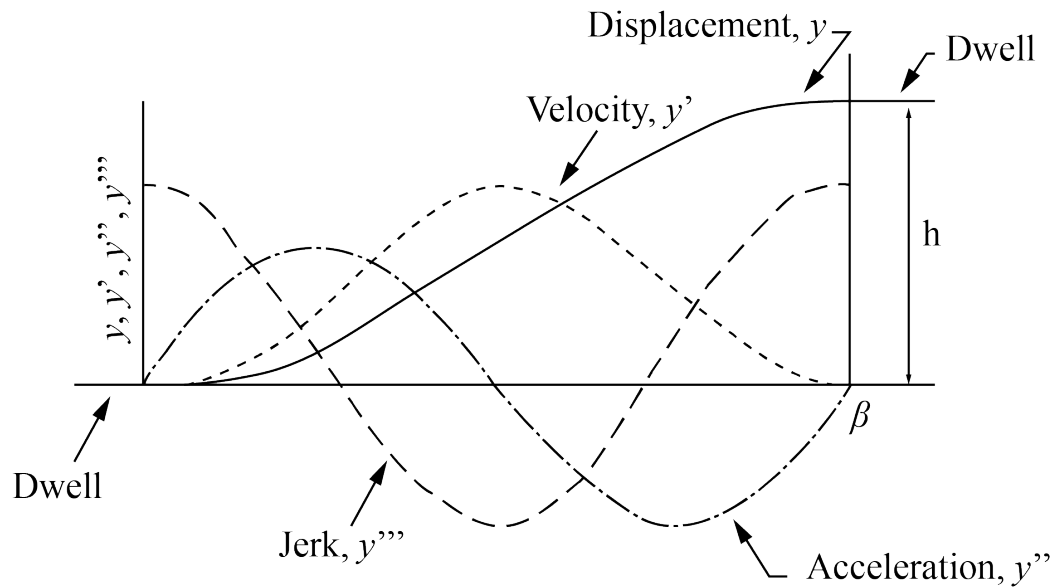


**Figure 1.2:** Basic cycloidal motion curves of displacement, velocity, acceleration, and jerk

In Figure 1.2, the various curves can be seen describing the dynamics of the system with respect to the follower as it travels over the surface of the cam based on the cycloidal equations of motion. Similar to the cycloidal displacement program, the

3-4-5 polynomial cam is often used as it offers both finite jerk and acceleration. The benefits of the 3-4-5 polynomial profile is that it offers a more gradual start and finish to the followers motion. This is ideal in high speed and high load applications as it helps to apply the load from the cam to the follower more gradually resulting in less wear than the cycloidal profile. The following equations represent the displacement, velocity, acceleration, and jerk profiles that are produced using a fifth order 3-4-5 polynomial cam displacement program.

Fifth Order 3-4-5 Polynomial Cam Profile: [1]

$$\text{Displacement} \quad y = 10L \left( \frac{\theta}{\beta} \right)^3 - 15L \left( \frac{\theta}{\beta} \right)^4 + 6L \left( \frac{\theta}{\beta} \right)^5 \quad (1.5)$$

$$\text{Velocity} \quad y' = \frac{30L}{\beta} \left[ \left( \frac{\theta}{\beta} \right)^2 - 2 \left( \frac{\theta}{\beta} \right)^3 + \left( \frac{\theta}{\beta} \right)^4 \right] \quad (1.6)$$

$$\text{Acceleration} \quad y'' = \frac{60L}{\beta^2} \left[ \left( \frac{\theta}{\beta} \right) - 2 \left( \frac{\theta}{\beta} \right)^2 + \left( \frac{\theta}{\beta} \right)^3 \right] \quad (1.7)$$

$$\text{Jerk} \quad y''' = \frac{60L}{\beta^3} \left[ 1 - 6 \left( \frac{\theta}{\beta} \right) + 6 \left( \frac{\theta}{\beta} \right)^2 \right] \quad (1.8)$$

The fifth order 3-4-5 polynomial is aptly named for the exponents that are seen on each term of the displacement expression. This results in the following displacement, velocity, acceleration, and jerk profiles seen in Figure 1.3. All polynomial displacement programs are based on odd order powers where first and third order polynomial programs offer little benefit, but fifth, seventh, and ninth order polynomial programs allow for more control over the way in which the follower transitions between dwells.

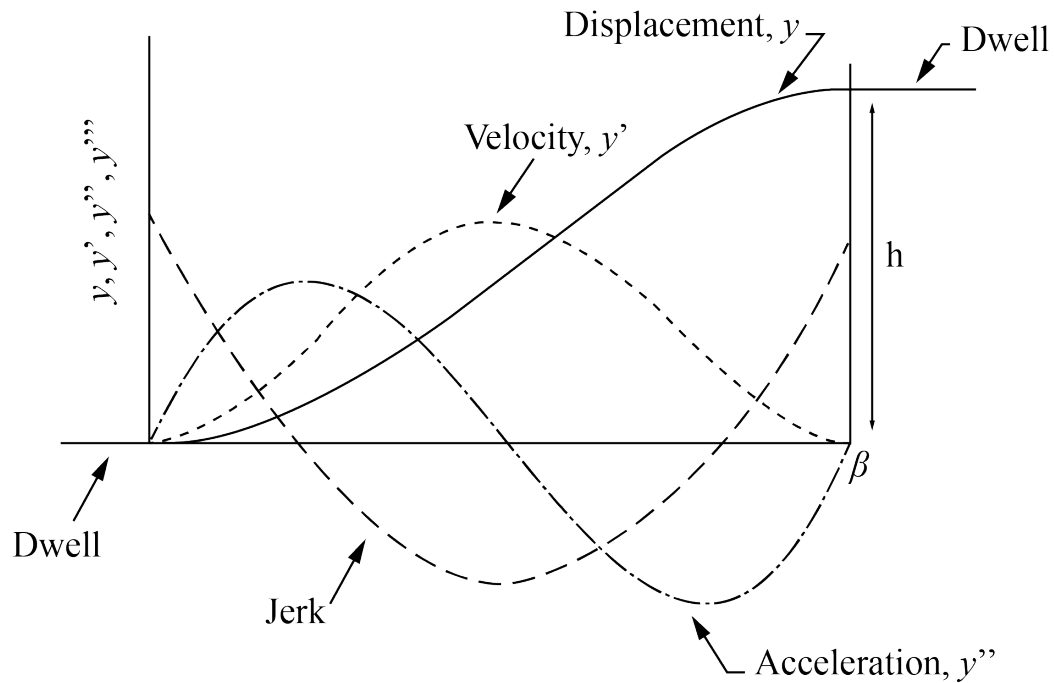


**Figure 1.3:** Basic 3-4-5 polynomial motion curves of displacement, velocity, acceleration, and jerk

Fifth and higher order odd numbered polynomial displacement programs, produce finite acceleration and jerk which provides a smooth operating cam with reduced wear characteristics. Although benefits can be seen when a seventh or ninth order polynomial profile is used, high accuracy during machining of a seventh or ninth order polynomial cam must be maintained in order to see these benefits and it often results in a greater machining cost [1-3]. Thus a cost benefit analysis needs to be carefully considered between the additional control and the increase in manufacturing cost.

Besides the rudimentary uniform motion profile, which is easily recognized by its constant slope, there is visually little difference in the various displacement programs. This can be seen when the equation of motion for each displacement program is compared as shown in Figure 1.4. More noticeable effects become apparent when the velocity, acceleration, and jerk profiles are compared. Even though the various

programs all produce the same amount of follower rise  $h$  in the same duration  $\beta$ , they are significantly different dynamically.

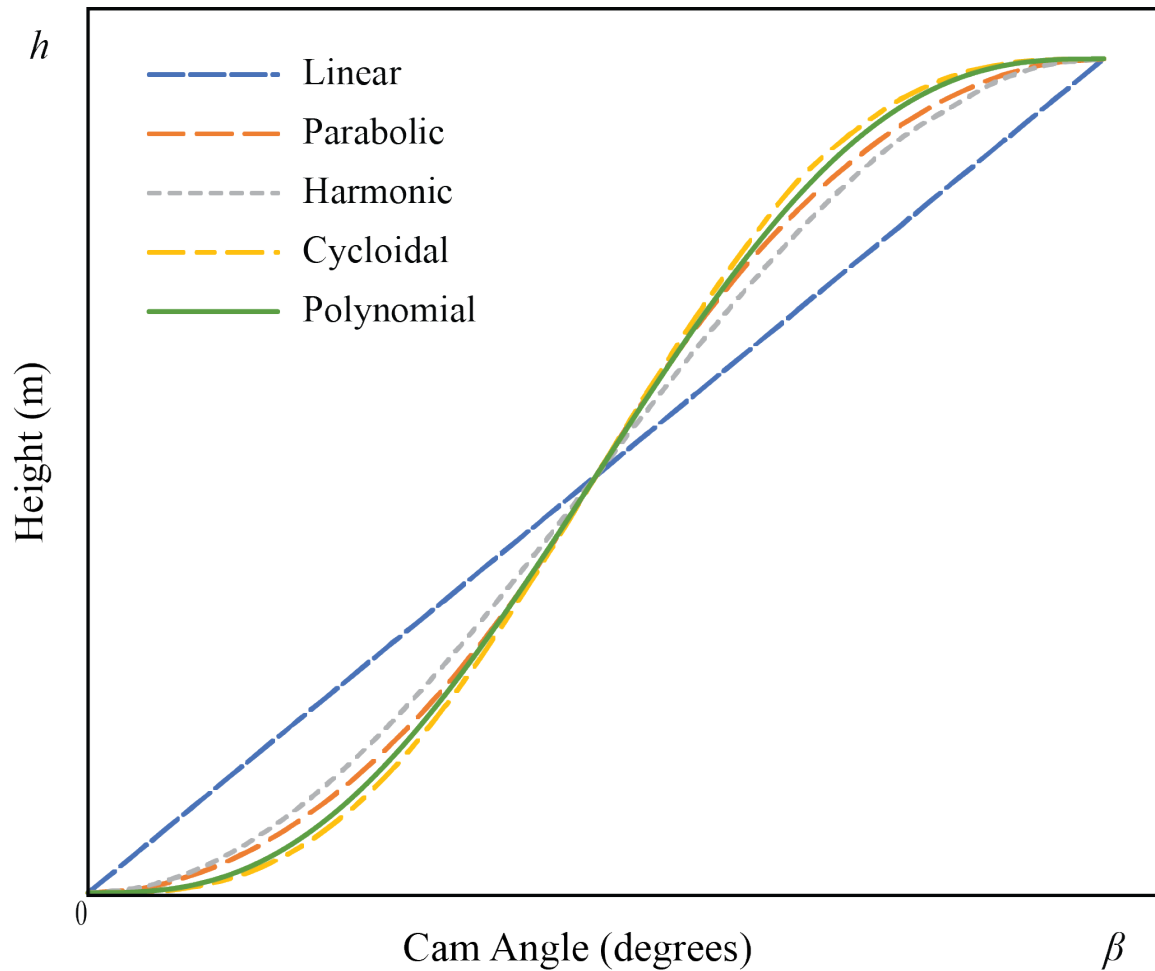


**Figure 1.4:** Comparison of common displacement programs considering follower rise  $h$  and duration  $\beta$

### 1.1.4 Torque

Understanding the torque requirements of the cam follower system are important for both sizing of the input motor or power demands depending on the means by which the cam is driven. The main distinguishing factors relate to the speed at which the cam is designed to be operated at. Much of this is due to the fact that the follower

velocity is a function of the rotational velocity of the cam. [1, 4]

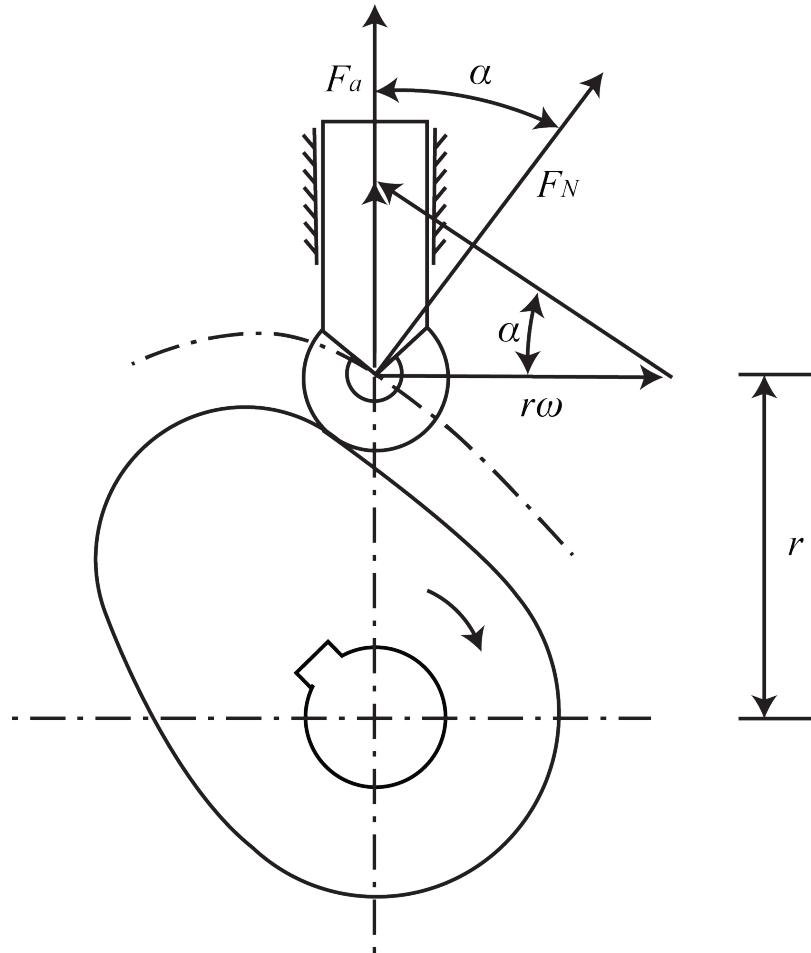


**Figure 1.5:** Free body diagram of a high speed cam

In a normal high speed cam with roller follower, the forces can be described as follows:

Normal component of velocity based on the known angular velocity of the cam:

$$N = r\omega \sin \alpha \quad (1.9)$$

The follower velocity(linear):

$$\dot{y} = r\omega \tan \alpha \quad (1.10)$$

The axial force applied by the cam to the follower:

$$F_a = F_n \cos \alpha \quad (1.11)$$

Since the lever arm  $r$ , is based on the distance between the cam and follower, the distance  $r$  changes with the cam's profile and the resulting torque can be described as:

$$T = rF_n \sin \alpha \quad (1.12)$$

By substituting the normal force from Equation (1.11) into Equation (1.12) the torque of the system can be represented by:

$$T = rF_a \tan \alpha \quad (1.13)$$

By then substituting the linear follower velocity Equation (1.1.4) into the Equation (1.12) for torque, the resulting equation becomes the torque as a function of the load on the follower  $F_a$ , the follower velocity  $\dot{y}$ , and the angular velocity of the cam  $\omega$ . This can be represented as:

$$T = \frac{F_a \dot{y}}{\omega} \quad (1.14)$$

$$= \frac{(F_a + m\ddot{y}) \dot{y}}{\omega} \quad (1.15)$$

When considering a very specific torque profile required to perform a certain task, the displacement, velocity, and acceleration requirements of the follower can be utilized

to create a more detailed torque profile. Ultimately, an understanding of the specific requirements of the cam profile along with the desired characteristics are essential in creating a cam follower system that produces the desired output.

## 1.2 Literature Review

The following portion of this thesis represents the literature in regards to the design of cams and the means by which the forces are transmitted to and from the cam profile. The majority of cam-follower research utilizes analytical models attempting to optimize cam profiles to minimize wear characteristics and reduce the required input energy. The first portion of this describes the current research in displacement programs along with suggested limits. The works following this, attempt to understand the most ideal way to optimize the operation of cam-follower systems focusing on which aspects of cam design are the most important during the design process. The subsequent sections consider the importance that pressure angle has on the design of a properly functioning cam-follower system and cam specific phenomenon that need to be considered. It is then concluded with current gaps in the literature followed by the objectives of this thesis.

### 1.2.1 Cam Synthesis

Cams have played an important role in much of early machinery as they were a way to produce a non-sinusoidal repeatable motion from a sinusoidal input. This led to a substantial amount of research into the design process of cam follower systems re-

sulting in several textbooks that are generally considered to be the current point of reference in modern cam design. Rothbart's Cam Design Handbook from 1965 has seen many revisions but is still one of the most detailed cam design manuals available today [1]. Chen's 1982 book titled Mechanics and Design of Cam Mechanisms is another reliable source commonly used and referenced in much of modern cam research and design [3]. They both describe the various cam and follower types along with the related dynamic and kinematic equations relating to them. Rothbart suggests that the maximum pressure angle should not exceed 30 degrees as it generates substantial lateral forces and increased wear characteristics. It is mentioned that testing had shown that pressure angles as high as 47.5 degrees with extremely small loads and over designed linkages had been tested [1]. This 30 degree pressure angle limit is generally reserved for radial cams with roller followers as other types of followers have different movement characteristics which lend themselves to alternative applications and their own respective limits. Even though designs aim to minimize pressure angle, it does not explain the reasoning behind the 30 degree limit.

Since many cam applications are subjected to high speed rotation, which is generally regarded as 4000-6000 RPM's, the acceleration and jerk characteristics of cam profiles are very important. In the 1980's many papers began to investigate wear characteristics and attempt to optimize cam design. MacCarthy and Burns consider the use of b spline functions in cam design [8]. With uniform motion extremely simplistic profiles are capable of the rise and fall required for the follower output but smooth operation at high speed is impossible due to the derivatives of the displacement and velocity profiles resulting in infinite acceleration or jerk. Thus the b spline



curve allows for smoother transitions at the beginning of the rise, the inflection point, and the end of the rise. In 1989 Sandgren and West further investigate the b spline curve using a nonlinear programming algorithm to optimize smaller portions of the displacement program [9]. In attempts to synthesize an optimal cam profile they attempted to impart selective control points within the displacement program prior to generating a spline based curve. From their study they had success with the optimization algorithm and were able to vary many of the given cam design parameters while optimizing the acceleration, jerk, and instances of negative radius profiles, yet there is no mention of the affects of pressure angle which will later be discussed as one of the most important parameters of cam design [9]. In 1993 Tsay and Huey discuss how the work of Rothbart and Chen can be improved by slightly modifying small portions of the polynomial and spline functions to reduce peaks in accelerations which is done by increasing values at other locations in the cam profile [10]. In 1993 Koon and Rao also investigated cam synthesis citing Tsay and Huey as well as Sandgren and West, arguing that a cubic spline function offers benefits over high order polynomial cam profiles [9–11]. They suggest that values of acceleration and jerk can be reduced when compared to those of polynomial functions. They do not consider some of the other requirements of cam design, which suggest the benefits they found, may be reduced in other aspects of the cam design process.

## 1.2.2 Selecting Cam Parameters

During the synthesis of a cam profile, the selection of various cam design parameters need to be considered in order to produce a cam follower design with minimal wear characteristics and smooth operation. In 2011 Silva et al. suggested that pressure angle is one of the most important design characteristics and give a means to synthesize a cam profile with the design being based on a pressure angle limit [5]. While pressure angle is an important design parameters it is effected by the base circle and follower radii, the type of displacement program that is selected, and the follower offset. In 1998 Yu and Lee looked into a method to optimize the size of the cam profile [12]. They suggested that since the displacement for a required cam profile is always a fixed value, the follower travel is just a function of the base circle radius. As the size of the base circle is increased the resulting pressure angle is decreased. As the base circle radius is increased, the rotational speed of the cam remains the same but the velocity at the surface is drastically increased. Therefore, if the follower radius is fixed, this results in more gradual changes which can reduce the lateral forces the cam is subjected to. Again, a nonlinear programming technique is used to slightly adapt the curvature in attempts to synthesize a cam profile with a reduced base circle diameter while staying within the given constraints for a specific range of pressure angles, acceleration, and jerk [12]. In 1996, Yan et al. analyzed the affects of cam speeds in radial cam-follower systems [13]. While the ability to control the rotational velocity of a cam may not be feasible in all applications experimental data showed that unfavorable velocity, acceleration, and jerk characteristics could be mitigated by

reducing the velocity during periods of rapid changes in displacement [14].

### 1.2.3 Design Limitation

Through the attempts to optimize the various aspects of cam design, the pressure angle always appears to have an effect. Pressure angle is most easily defined as the angle between the axis of transmission and the motion of the follower. This provides an extremely important role in the force transmission, as it determines how much of the applied torque is converted to axial and lateral forces. In 2011 Silva et al. discuss how the pressure angle is a function of the prime circle radius and the cam angle. [5] Thus, in attempts to solve this single equation with two unknowns, geometric relationships were determined to approximate the pressure angle  $\alpha$  as a function of the prime circle radius  $R_p$  and the range  $\beta$ . By developing these various relationships for the different displacement programs an analytical solution capable of approximating the prior method of numerical iteration was determined. This was extremely important as the overall size of the cam and the pressure angle are suggested to be two of the major contributing factors of an efficient cam design according to Rothbart, Chen, Uicker, Koomok, and Norton. [1,3,7,15,16] Not only do these authors all suggest that pressure angles should be restricted to 30 degrees or less for radial cam-follower systems but that the overall efficient operation relies on the pressure angle being as small as possible while limiting the size of the cam. As cam size is increased the inertia becomes an issue when the dynamic properties of the cam are considered. [1,3,15,16] Since the pressure angle is related to the change in cam radius

relative to the change in cam rotation, increasing the base circle diameter and pitch profile respectively, it is possible to produce the same linear motion in the same given amount of rotation with a smaller pressure angle.

### **Pressure Angle Limitations**

Rothbart's Cam Design Handbook provides a detailed explanation of the means by which forces are transferred between the cam and follower including the torque, friction, and inertia experienced by the various components, as well as how pressure angle is an important design concern [1]. As the previous section suggests, increasing the overall radius  $R_p$  of the cam should result in a better cam design as it reduces pressure angle and minimizes these unwanted forces [5]. While the literature suggests many limitations of various cam and follower combinations, which for radial cams with roller follower states a maximum 30 degree pressure angle for efficient operation, the 30 degree pressure angle stipulation appears to be considered as the maximum in the various literature with no regard as to why [1, 2, 4, 7, 16–18]. Rothbart [1] mentions increasing the pressure angle as high as 47.5 percent but does not discuss the outcomes except for the fact that a case with such a high pressure angle should be limited to minimal forces to minimize wear and potential damage to the various components. Other authors such as Norton, Koomok, Uicker, and Chen all propose the limitation of 30 degrees as well, without justification as to why. [1–3, 16]

### 1.2.4 Cam Phenomenon

Rothbart and Koster [1, 19] have both noticed an interesting phenomenon that occurs when pushing the design limits of cam follower design. The two main phenomenon are shaft windup and follower jump. Shaft wind up is where the actual speed of the cam does not maintain a constant velocity due to twisting of the shaft. [1, 19] Using a high speed camera, Rothbart was able to observe this phenomenon as the input shaft and the cam begin to rotate and differing speeds due to the loads being applied to them. This results in undesirable vibration within the system as the shaft twists, acting like a spring. The cam shaft elasticity appears to be only a concern in systems where large cam shafts are used with high loads and undersized shafts but it is also important to note that Koster considers the follower deflection in his models as previous studies done by Bloom and Radcliff which assume the follower to be infinitely stiff. [19] The jump phenomenon occurs when the inertia of the follower causes it to lift off the cam resulting in the follower bouncing often causing catastrophic failure of the follower bearing. [1, 3] This can be mitigated by knowing the speeds the cam is designed to be operated at while also the correctly sized spring in order to maintain the contact between the cam and follower. While these phenomenon are both undesirable, their effects can be accounted for in the design process.

## 1.3 Gaps in Current Literature

The study of force transfer in cam follower systems has been extensively covered within the commonly discussed limits to create the most efficiently operating cam

follower systems. Through the study of cams in traditional applications, there seems to be agreement on the major limiting factors. In attempts to optimize these systems, the majority of research has focused on the synthesis of various profiles within the given limits and have attempted to produce various equations and methods by which the pressure angle, overall size, and displacement program can be determined to produce the most optimal cam profile. Various authors have attempted to produce cam profiles with slight advantages through means of displacement program modification, and design process optimization. Yet the research only ever considers the forces the cam imparts on the follower and the spring force require to prevent follower jump or excess vibration. It does not take into consideration instances of high follower load imparting forces on the cam during the fall.

Based on the review of current literature, there has yet to be any consideration for the recovery of energy that may be potentially recovered from residual loading of the follower. There is also very little understanding of the suggested 30 degree pressure angle limitation, and it has been accepted as a design limitation by many authors. Traditionally, cam follower systems have been a means to transform rotational motion into linear motion in the most effective means possible, yet with efficiency being an ongoing consideration, the potential to recover energy from the system should be considered. An analytical and experimental investigation of the potential for recovering energy from a cam follower system, along with a better understanding of the limitations of pressure angle, could provide a way to effectively leverage the use of cams in new or existing applications. While a high torque input is often required, the energy stored in the follower or produced by the reaction force could potentially

be harvested to limit the parasitic losses a cam imparts on a system.

## 1.4 Thesis Objectives

The objectives of this thesis are to analytically and experimentally determine the limitations of pressure angle in low speed cam designs, which is widely accepted to be 30 degrees. It also describes the means by which energy can be recovered from a cam follower system and what effects pressure angle may have on it. Thus, the main objectives are to:

- Develop a model to better understand the potential for energy recovery in attempts to limit the parasitic losses imparted by the cam and follower on the system.
- Design an experimental setup to determine whether the 30 degree pressure angle limit is a physical limitation for radial cams with roller followers.

## Chapter 2

# Experimental Apparatus and Methods

The following chapter discusses the design and testing of the experimental apparatuses used to accomplish the objectives of this thesis. To accurately test cam profiles and understand how the forces are distributed required the following:

- (i) Produce a variable and known force from the follower onto the cam profile
- (ii) Measure the lateral force produced by the follower with a known cam angle
- (iii) Accurately measure static and dynamic forces at various points of the profile
- (iv) Accurately measure the torque generated by the follower on the cam profile)



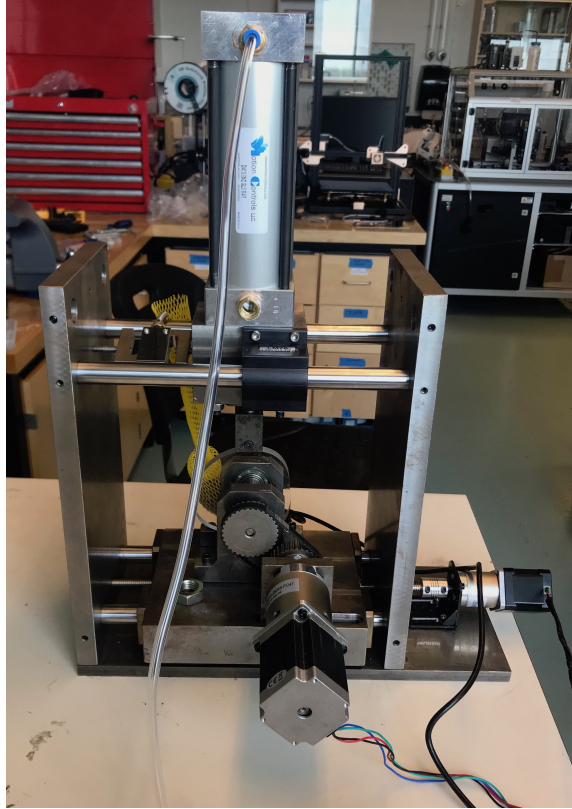
## 2.1 Apparatus Overview

The following section describes the design and fabrication of the dynamic and static test apparatuses used to accomplish the objectives of this thesis. It is assumed that the following testing is done using forces less than 150N and the rotational speed of the cam profiles tested are less than 50 RPMs due to the limitations of the motors being used. It is also assumed that friction is negligible as quality roller and linear bearings were used to minimize friction as much as possible.

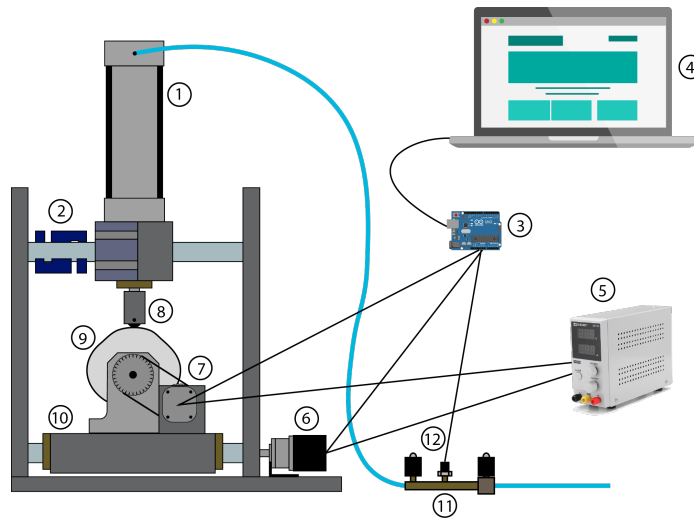
### 2.1.1 Dynamic Test Apparatus

The photograph and schematic in Figure 2.1, represent the dynamic cam-follower test apparatus. A NEMA 23 stepper motor with a 47:1 planetary reduction gear box was used to rotate the the cam profile that was being tested. In order to maintain sufficient torque output, the stepper motor was limited to 500rpm which was then reduced by the planetary gearbox to 10.6 RPM. Using a known starting location referenced off the keyway in the shaft, the offset, between the cam and follower could be set and locked in place using the acme shaft controlled by a secondary stepper motor. A pressure transducer utilized in conjunction with two solenoid valves allowed the various pressures to be set and regulated. An S type load cell located between the frame and pneumatic cylinder provided the lateral force measurement in order to better understand the relationship between the pressure angle and undesirable loading characteristics seen by the follower. The frame of the test apparatus was machined from 0.75 inch mild steel. The test bed to which the cam profile was suspended and

rotated on was supported by four 300lb dynamic or 600 lb static rated linear bearing with 0 degrees of self alignment, sliding on a pair of 0.75 inch diameter high carbon linear bearing shafts. These were chosen for their accuracy and ability to handle loads substantially over anything the cam test apparatus would operate at. In attempts to produce minimal error, the support structure was designed with a significant factor of safety in order to mitigate error with consideration of component costs. A 100kg s-type load cell was mount between the upper pneumatic cylinder support and the frame of the test apparatus. The pneumatic cylinder was suspended on two rails with linear bearings rated for 500lbs of dynamic and 750 lbs of static load with 0 degrees of self alignment in order to prevent deflection of the pneumatic cylinders shaft which acted as the follower arm for the system. Minimizing deflection and having a low friction means by which to transfer force to the frame, would allow for accurate lateral force measurements. The initial design utilized a NEMA 19 stepper motor with a 51:1 planetary gear box. A trapezoidal toothed pulley was mounted to both the shaft supporting the cam and the gearbox of the stepper motor. This was connected in a 1:1 configuration with a high tension belt in order to transfer the power from the motor to the cam. It is also important to note that the follower shaft is kept at the shortest possible length to minimize deflection and the shaft the cam is mounted to is substantially over sized to mitigate the effects of cam windup.



(a)



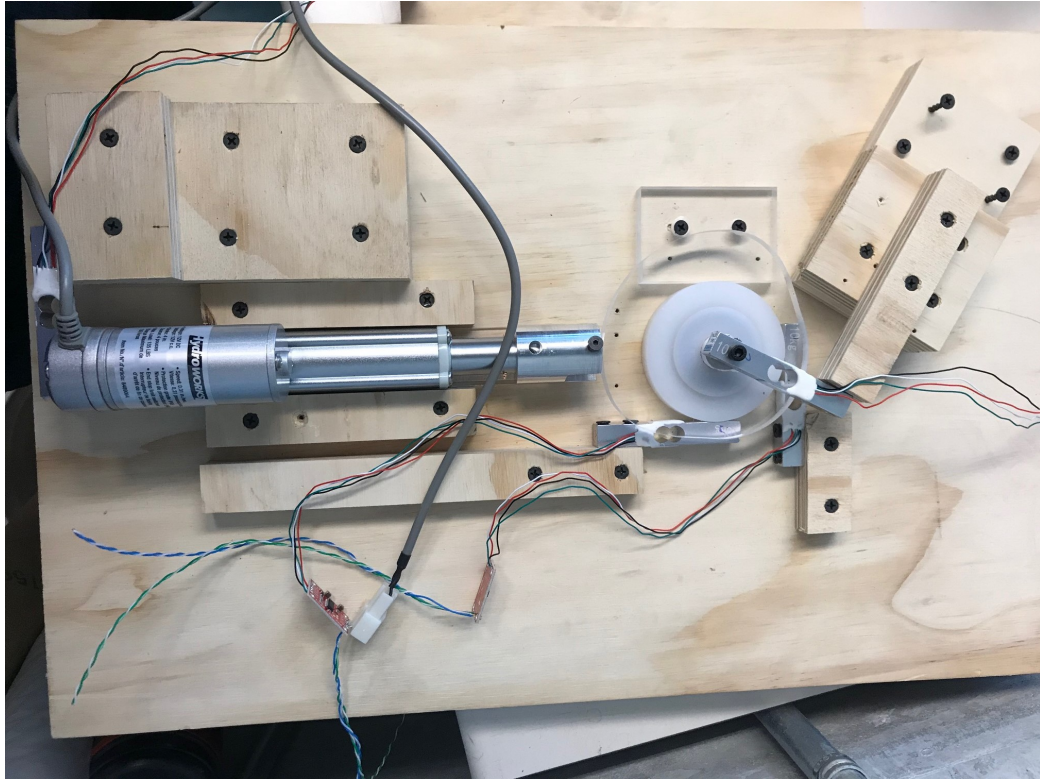
(b)

**Figure 2.1:** a) Photo of dynamic test apparatus b) Schematic of Experimental Setup: 1)pneumatic cylinder, 2)load cell, 3)Arduino, 4)laptop, 5)power supply, 6)NEMA 19 stepper motor, 7)NEMA 23 stepper motor and gearbox, 8) follower, 9)cam profile, 10)adjustable offset base, 11)pressure regulator, 12)pressure transducer

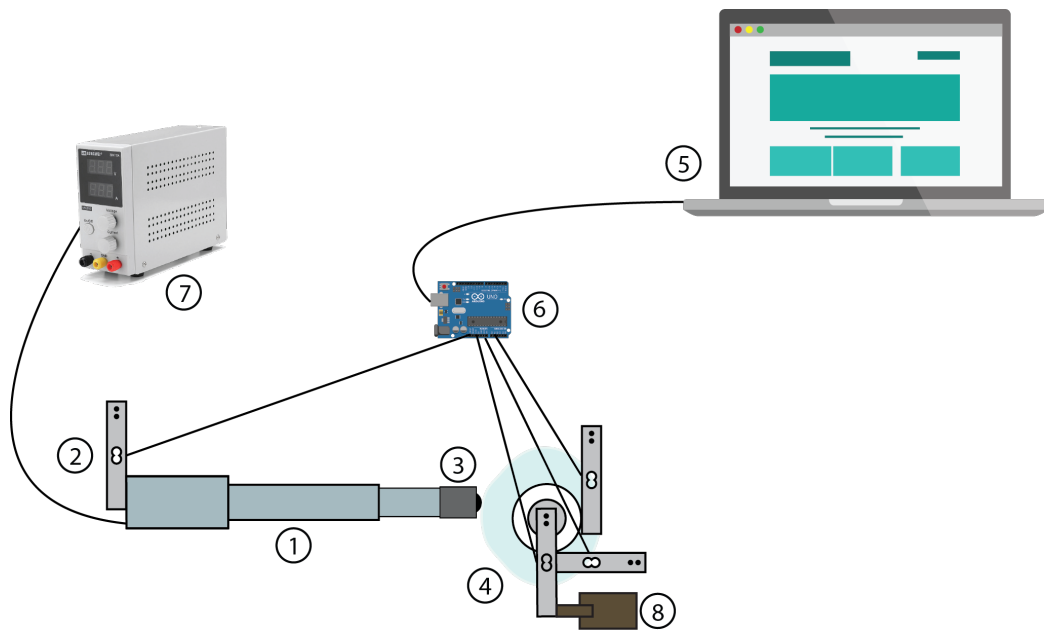
### 2.1.2 Static Test Apparatus

The static test apparatus was used in two different configuration in order to understand how the forces and torque changed. The fixed position configuration applied the force to the cam while it remained stationary. The second configuration offered a variable cam position by utilizing a spring positioned between a moment arm of known length and a fixed stop. Using a linear actuator force was gradually applied while the X-component, Y-component, and torque(via the load applied to the end of the moment arm) were recorded. This provided a known applied force by the linear actuator as well as the components of force that were seen by the cam. By holding the cam in a fixed position as seen in the photograph and schematic in Figure 2.2, the distance  $r$  which represents the distance between the cam center and follower center could chosen by moving the fixed base. This provided a way to measure the increase in torque due to the increase in applied load while holding all other variables constant. The second configuration used a spring placed between the moment arm and a fixed based as seen in the photograph and schematic in Figure 2.3. This provided the ability to observe how the X-component and Y-components were effected as a direct result of the increase in torque provided by the resistive force of the spring. The static cam tester was constructed from plywood for dimensional stability and utilizes a 110 lb force (490.5 N) linear actuator to apply the load. The four 10 kg load cells were calibrated before being installed. A bearing was placed into a high density polyethylene (HDPE) bushing to allow it to slide with minimal friction while providing enough support for the shaft. The linear actuator was also placed inside

of a guide with a HDPE strip underneath to allow the linear actuator to not only apply load to the cam but to measure the axial force being applied. This allowed the forces applied to the cam to be recorded relative to the applied force while tracking the torque that is generated in both cases.

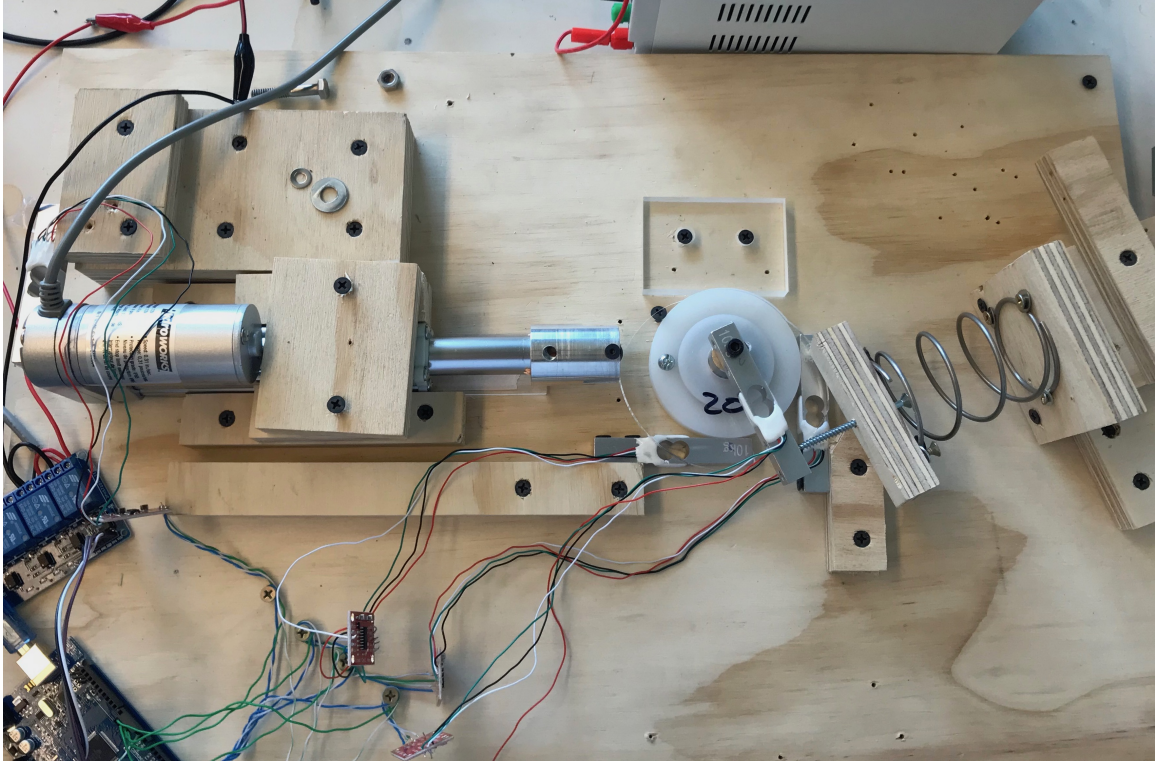


(a)

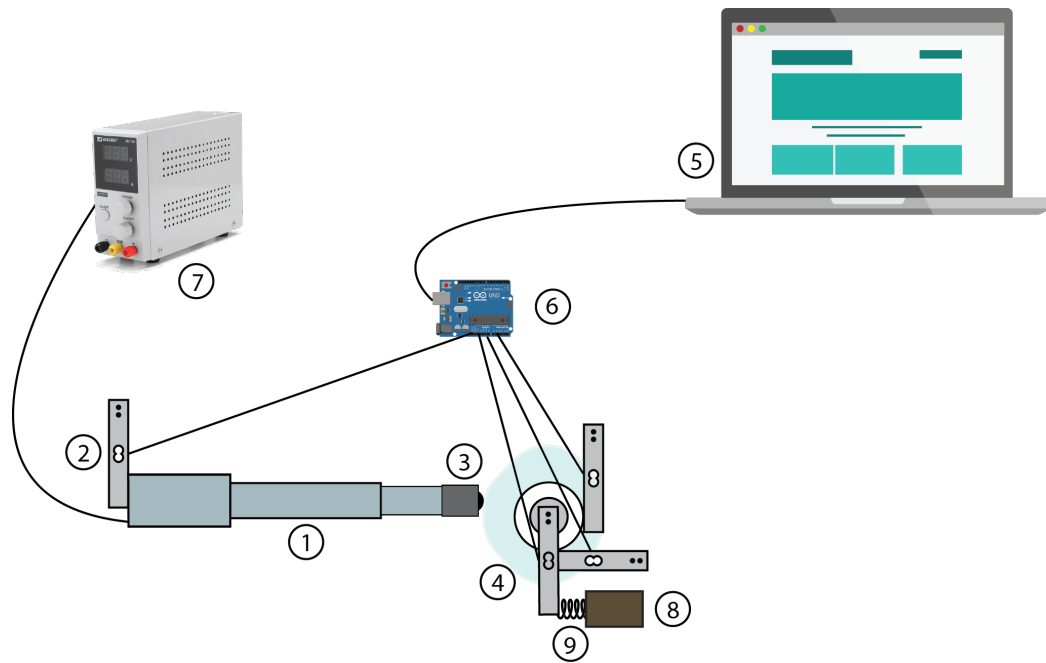


(b)

**Figure 2.2:** A) Photo of static test apparatus with fixed cam b) Static force tester schematic with fixed cam placement: 1) linear actuator, 2) load cell, 3) follower, 4) cam, 5) laptop, 6) Arduino, 7) power supply 8) adjustable stop



(a)



(b)

**Figure 2.3:** a) Photo of static force tester with variable cam angle and sprung moment arm b) Static force tester schematic with fixed cam placement: 1) linear actuator, 2) load cell, 3) cam profile, 4) follower, 5)laptop, 6) Arduino, 7) power supply 8) adjustable stop, 9) spring

## 2.2 Uncertainty and Sources of Error

### 2.2.1 Dynamic Cam Tester Error

During the designing of this test apparatus, the required torque was uncertain as the pressure angle, and applied forces would be varied, as well as the size of the cam profiles to be tested. The NEMA 19 stepper motor with a 51:1 gear box was eventually discovered to be undersized and replaced by a larger NEMA 23 stepper motor with a 47:1 planetary gear box. This proved to be sufficient for pressure angles less than 45 degrees when the applied force was less than 125 N. If the pressure angle or force was increased and the required torque demand was exceeded the motor speed would slow down and occasionally steps would be missed. The 23HS30-2804S-PG47 NEMA 23 stepper motor with 47:1 planetary gear reduction is a 200 step stepper motor with a  $\pm 0.5$  degrees of accuracy. The Arduino code written to control the stepper motor divides the 200 steps into 360 degrees and then compensates for the gearbox reduction. This results in 1 degree of output rotation being equivalent to 26.1 steps of input. As stepper motor speed increases the torque output is reduced by upwards of 50% which is undesirable. In attempts to more accurately measure the rotation, micro-stepping was considered which also reduces the output torque of the stepper motor by as much as 30% or more, depending upon the degree of micro-stepping. Due to this, 26 steps was approximated as 1 degree which equates to 99.57% of a degree or an error of 0.43%. The load cell used in this test was a 100 kg s type load cell with a error  $\pm 0.7\%$ . This was calibrated using known masses of 1, 3, 5, 10, and 15 kg with an average error of 2.4%. While the fasteners used



to mount the load cell between the frame and follower/pneumatic cylinder are small in diameter the amount of stretch based on the foreseen loads was determined to be negligible. The 1.2 MPa pressure transducer used to regulate the cylinder pressure has a listed error of 1.5%. A major concern was the friction caused by the seal within the pneumatic cylinder. After ensuring the piston was correctly lubricated, the pressure was gradually increase from 0 until the piston began to move and the pressure was also decrease from a high pressure until the piston stopped moving. This resulted in 1.85 psi and 2.05 psi respectively. During testing a minimum of 3 psi was used to ensure that the follower would maintain contact with the cam profile without risk of the follower hanging as the cam profile transitioned from a dwell to a fall. The pressure in the pneumatic cylinder was measured during each step and compared to the desired pressure, which reached a maximum error of 0.3%. Ignoring the friction loss from the pneumatic cylinder, the overall error was considered to be  $\pm 4.9\%$ . Since the pressure angle of the cam was known and a relation of applied force to lateral force was known, the theoretical applied force could be determined with a reasonable amount of confidence.

### 2.2.2 Static Cam Tester

The static cam tester utilized a number of bar type 10 kg load cells with a rated combined error of 0.5%. These load cells were then calibrated by fixing them to a surface with the provided mounting locations. Masses of 50 g, 250 g, 500 g, 1000 g, and 2500 g were measured using an AccuWeight food scale with a listed error

of 0.8% before they were suspended from the load cells. The linear multiplier used in the Arduino program to convert the analog signal was then determined and the masses were measured 3 times with a measured average error of 1.4% resulting in a total of 1.45%. Since the X-component, Y-component, and torque were based on the known input force from a load cell attached at the back of a linear actuator the total measurement error is approximately  $\pm 4.15\%$ .

In order to minimize the amount of friction between the components and the plywood substructure, pieces of HDPE were used to reduce the friction, allowing components to more accurately transfer the forces. Engineering texts seem to agree that steel on wood results in a friction factor of approximately 0.6 whereas steel on HDPE is approximately 0.2 [2]. Since the components are static, and in the sprung case the steel shaft is mounted inside of a bearing, friction was considered to be negligible.

### 2.2.3 Round Profile Test

In order to ensure the cam tester was properly aligned and the forces were being transferred correctly, a circular profile was tested using 150 g, 250 g, and 500 g applied loads as measured by the load cell labeled 2, in Figure 2.2. The X-component(lateral), Y-component(Axial), and torque on the circular profile was then compared to the applied load. Since the circular profile results in a pressure angle of zero degrees the resulting components should theoretically result in a completely axial transfer. Three trials were completed for each of the 150 g, 250 g, and 500 g loads with the nearest

points to 25%, 50%, 75%, and 100% of the applied load being plotted. Slight lateral forces were measured resulting in the test apparatus being realigned. From Figure 2.4, it can be seen that when the cam profile has a 0 degree pressure angle the applied force is transferred axially through the cam profile with no torque being generated.

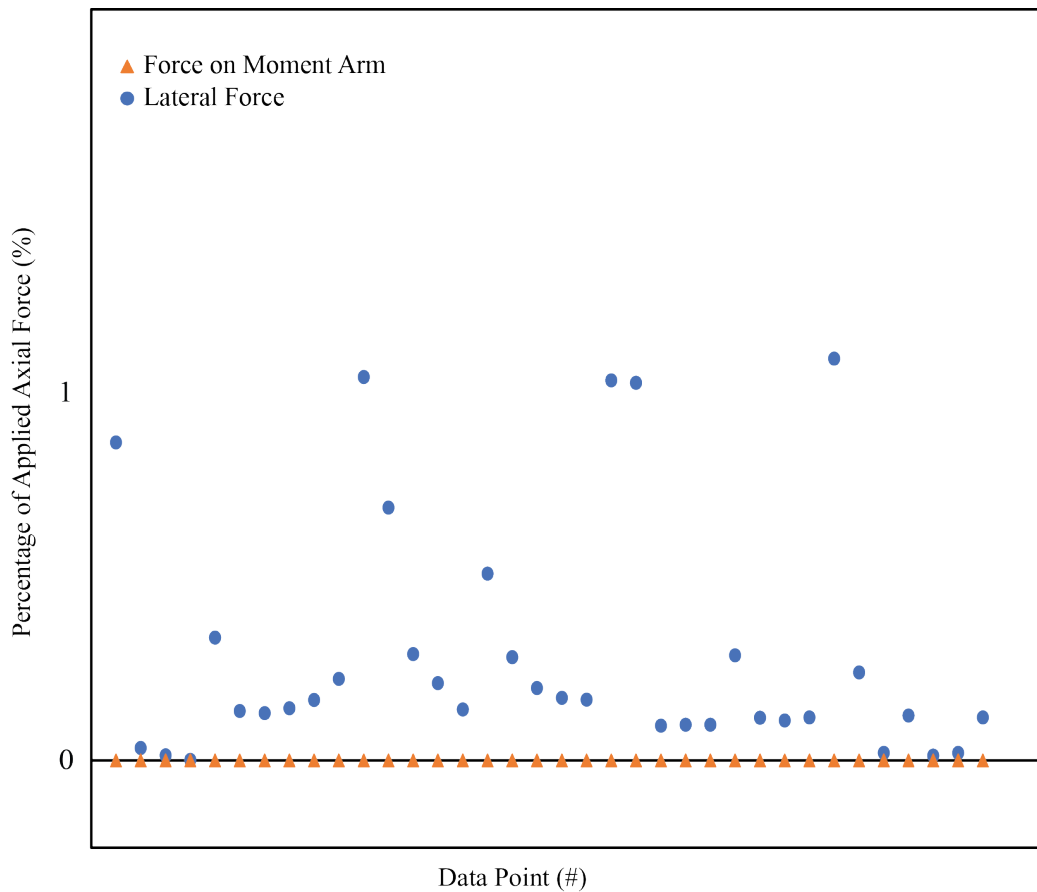


**Figure 2.4:** Distribution of forces as a percentage of the applied load on a circular cam profile

It is also noted that from the 36 readings taken during the post alignment tests, the mean lateral force was 0.32% of the applied load. This error is considered acceptable as it is less than the noted error for the load cells. The few points in Figure 2.4 that approach 1% are attributed to the misalignment caused by slight deflection in the test setup and considered negligible.

## 2.3 Experimental Method

The following method was utilized to perform the experiment in attempts to minimize all sources of error and ensure repeatability.

### 2.3.1 Dynamic Cam Tester Procedure

All wiring was checked prior to applying 12VDC to the relay board. The Arduino program was uploaded and communication was checked. The python script was then run, a file name was selected, the cam offset, and cam zero position were set. The pressure was bled off from the system and the follower was backed off to ensure the load cell could be properly tared before beginning the test. The number of revolutions was then set and the pressure profile that provided the axial force was set. Once all of the parameters had been initialized the start sequence was initiated. The test apparatus would then proceed to regulate the pressure in the cylinder to provide a measurable applied axial force while measuring the lateral reaction force at each incremented step of the cams revolution. Each test was run multiple times with a minimum of 2 revolutions to ensure oddities in the data could be better understood.

### 2.3.2 Static Cam Tester Fixed Position Procedure

The linear actuator was checked to ensure it was freely able to move along the axial direction. The cam was slightly rotated to ensure the load cell was not contacting any of the surfaces allowing it to properly tare when the program was initiated. The power supply would be set to 12VDC and the Python program would then communicate

with the Arduino to tare the load cells before increasing the applied force until the set limit was reached. The linear actuator would be activated for 50ms at a time gradually increasing the applied force while measuring the components and torque produced at the cam.

### **2.3.3 Static Cam Tester Variable Position Procedure**

Unlike the fixed position test, the load cell attached at the cam center used to measure the torque, was attached to a spring with a known spring rate. The same procedure as the fixed position test was followed but with the cam able to rotate due to the spring being located between the load cell and the fixed point.

# Chapter 3

## Results and Discussion

The following chapter discusses the analytical findings regarding the potential of energy recovery in regards to the required input torque and available output torque in a low speed radial cam and roller follower based system. It also discusses the findings based on the experiments conducted using both the dynamic and static cam test apparatuses as previously discussed in regards to the limitations of pressure angle.

### 3.1 Comparison of Torque Forces

From the previous research, cam follower systems were either utilized solely as a means to convert rotational motion into linear motion, or to use energy stored in a spring or gas strut to partially rotate a cam profile in order to move an object with a known force requirement. This suggests that in situations where the follower load varies, there is potential to both drive the cam via an input to perform a desired task while also being able to recover energy from the follower. Optimizing this energy recovery

then becomes a question of cam profile shape and what the pressure angle should be. Figure 3.1 represents the free body diagrams of the cam follower mechanism as an input torque rotates the cam pushing the follower upwards. Intuitively the torque applied to the cam profile exerts a force normal to the cam where it contacts the follower. This is then split into an axial and lateral component. Since the moment arm is the distance  $r$  between the cam center and follower center, the axial force the follower sees  $F_a$  can be easily determined from the input torque  $T_{rise}$  during the rise. The normal force  $F_n$  represents the force transferred to the follower by the cam along the axis of transmission. This can be described as:

$$\cos \alpha = \frac{F_a}{F_n} \rightarrow F_n = \frac{F_a}{\cos \alpha} \quad (3.1)$$

The lateral component  $F_l$  of the normal force  $f_n$  can then be written as:

$$\sin \alpha = \frac{F_l}{F_n} \rightarrow F_l = F_n \sin \alpha \quad (3.2)$$

This results in a relation for the torque needed to raise the follower based on a given pressure angle  $\alpha$ , known center to center distance  $r$ , and required axial force  $F_a$ :

$$T_{rise} = r F_n \sin \alpha = r \frac{F_a \sin \alpha}{\cos \alpha} = r F_a \tan \alpha \quad (3.3)$$

This also provides the ability to easily determine the axial force  $F_a$  the cam imparts on the follower based on a known torque  $T_{rise}$  and pressure angle  $\alpha$ :

$$F_a = \frac{T_{rise}}{r \tan \alpha} \quad (3.4)$$

Once the follower reaches the dwell portion, assuming minimal friction, the pressure angle being 0 suggests that the entire force  $F_a$  pushing back on the cam is directly passed through the center shaft of the cam when there is no offset. This results in the input torque only having to overcome the friction between the bearing on the roller follower and polished cam surface.

Assuming there is a device capable of perfectly storing the energy the cam imparts on the follower during the rise, the cam should then be able to recover that energy during the fall by reversing the process.

As shown in Figure 3.1 when comparing the free body diagram of the output torque  $T_{fall}$  to that of the input torque  $T_{rise}$ , the energy stored in the follower is returned to the cam through the follower but the output torque is not equivalent to that of the input torque. This is due to the largest component of the force triangle being  $F_a$  and not  $F_n$ .



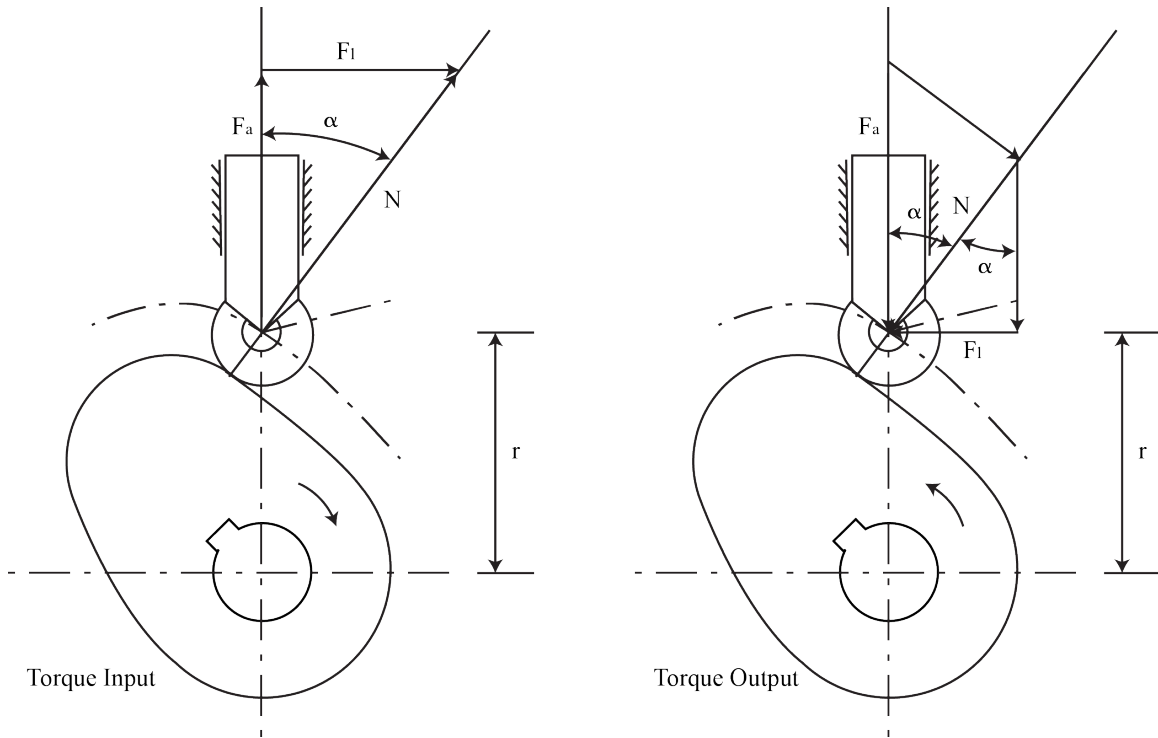


**Figure 3.1:** Comparison of forces when comparing torque applied to a cam and torque imparted on a cam by the follower

This results in an output torque that can be described as follows:

The normal force is now a function of the applied force that was stored and returned through the follower as:

$$\cos \alpha = \frac{F_n}{F_a} \rightarrow F_n = F_a \cos \alpha \quad (3.5)$$

The lateral force is a function of the normal force:

$$\sin \alpha = \frac{F_l}{F_n} \rightarrow F_l = F_n \sin \alpha \quad (3.6)$$

The output torque similar to the input torque still remains a function of  $r$ ,  $F_a$ , and

$\alpha$ :

$$T_{fall} = rF_l = rF_n \sin \alpha = rF_a \sin \alpha \cos \alpha \quad (3.7)$$

From this it can be concluded that the torque is always a function of the moment arm  $r$ , the desired axial force at the follower/available energy stored in the follower  $F_a$ , and the pressure angle  $\alpha$ . If the input torque  $T_{rise}$  and the output torque  $T_{fall}$  are written as a ratio the resulting relation can be determined:

$$\frac{T_{fall}}{T_{rise}} = \frac{rF_a \sin \alpha \cos \alpha}{rF_a \tan \alpha} = \cos^2 \alpha \quad (3.8)$$

By plotting the input and output torque as a function of pressure angle, Figure 3.2 shows that by reducing the pressure angle, a smaller amount of input torque is required to apply an equivalent axial force  $F_a$  on the follower. Interestingly, the output torque is maximized at a 45 degree pressure angle which results in a maximum of 50% of the applied force from the follower  $F_a$  being converted into lateral force  $F_l$  capable of producing torque. As the pressure angle is decreased or increased from 45 degrees the system becomes less efficient at producing output torque. According to Equation (3.8), the output torque is maximized as the pressure angle is decreased.

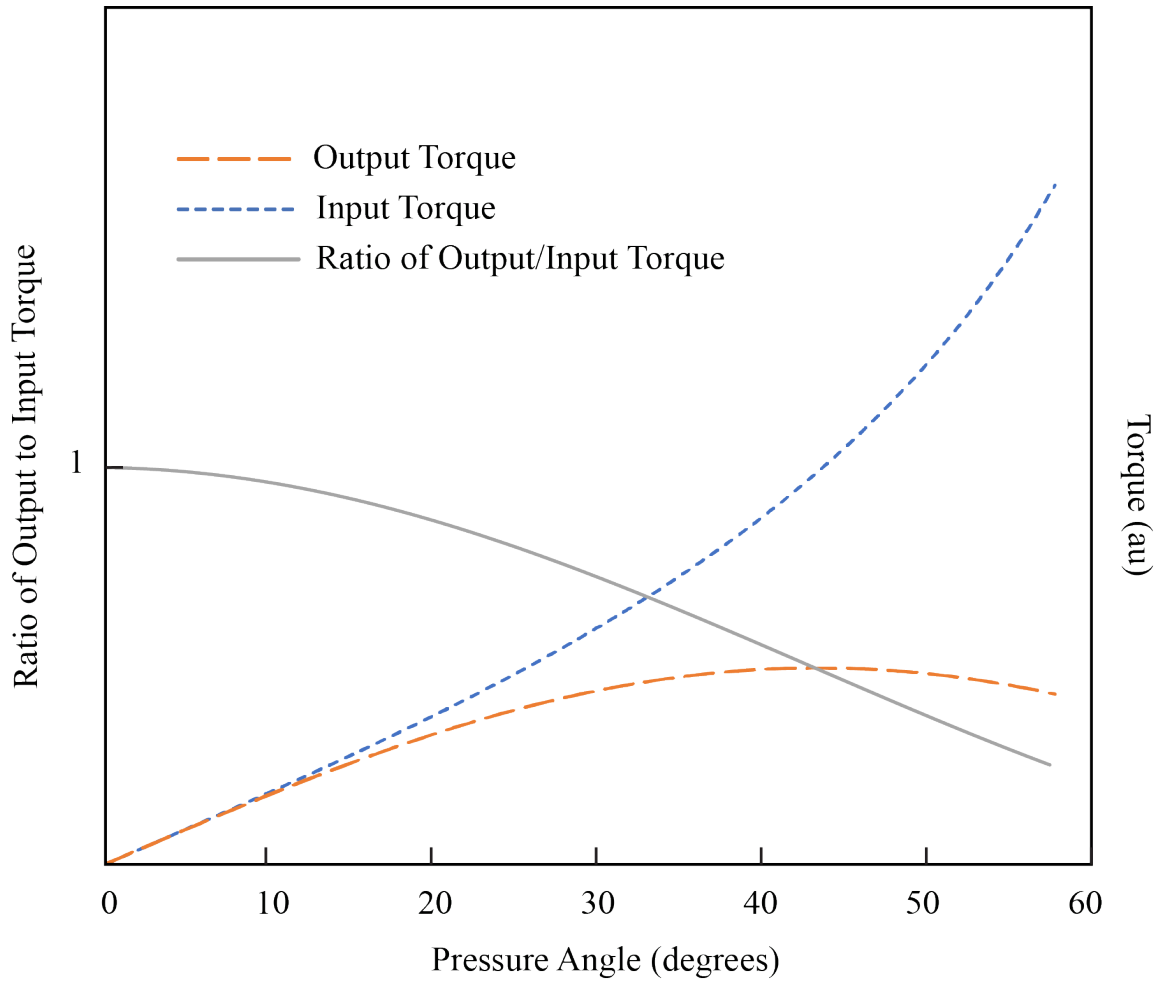


**Figure 3.2:** Input and output torque as a function of pressure angle including the respective ratio of output torque to input torque

As the follower rises from the lowest point on the cam profile to the highest point, the distance between the cam center and follower center  $r$  increases with cam angle  $\theta$ . In a uniform motion displacement program this results in a fixed pressure angle which can be used to better understand how the  $T$ ,  $r$ , and  $F_a$  are affected. If a constant force of  $F_a$  is required we can see from Figure 3.3, the required torque increases with both the pressure angle and cam angle. As the pressure angle is increased the amount of duration  $\beta$  is decreased. The resulting area under each curve is equivalent which means the amount of energy that can be extracted given the same rotational velocity

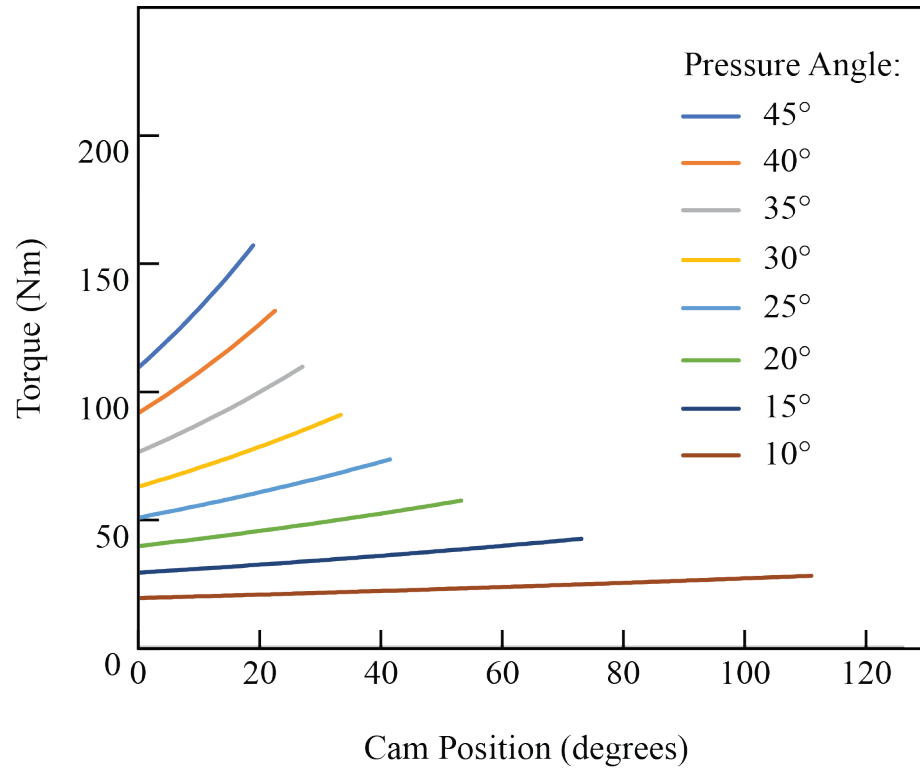


**Figure 3.3:** Input torque relative to pressure angle assuming unit radius  $r$  and unit force  $F_a$

is equivalent. Using Equation (3.8), as the pressure angle is increased from 0 to 45 degrees the amount of maximum recoverable energy is halved. Therefore to minimize the input torque required while maximizing the amount of recoverable energy, the pressure angle needs to be kept as small as possible. The trade off is that as the pressure angle is decreased, the duration  $\beta$  of the rise/fall is increased.

## 3.2 Pressure Angle Limitations

The pressure angle plays an important role in the understanding of how the forces are transmitted between the cam and follower as well as those from the follower to the cam. As discussed in the previous section, during the rise, the cam is driven and the

follower is subjected to lateral and axial components of the force based on the pressure angle. During the fall, the force distribution is different as the maximum applied force comes from the follower and not the normal, even though the pressure angle could be the same. This suggests that the pressure angle limits during the rise and fall portions may be very different even for symmetrical cam profiles. From Figure 3.4 it can be seen that when a 30 degree pressure angle is utilized the lateral force experienced by the follower becomes 50% of the applied force, while the axial force component is 86.6%. As the pressure angle is increased to 45 degrees the axial and lateral force components become equivalent at 70.7%. This provides little understanding as to why the maximum pressure angle is chosen to be 30 degrees when designing these systems. Therefore there is a need to test profiles which exceeded the 30 degree pressure angle limit in order to determine what effects they result in.

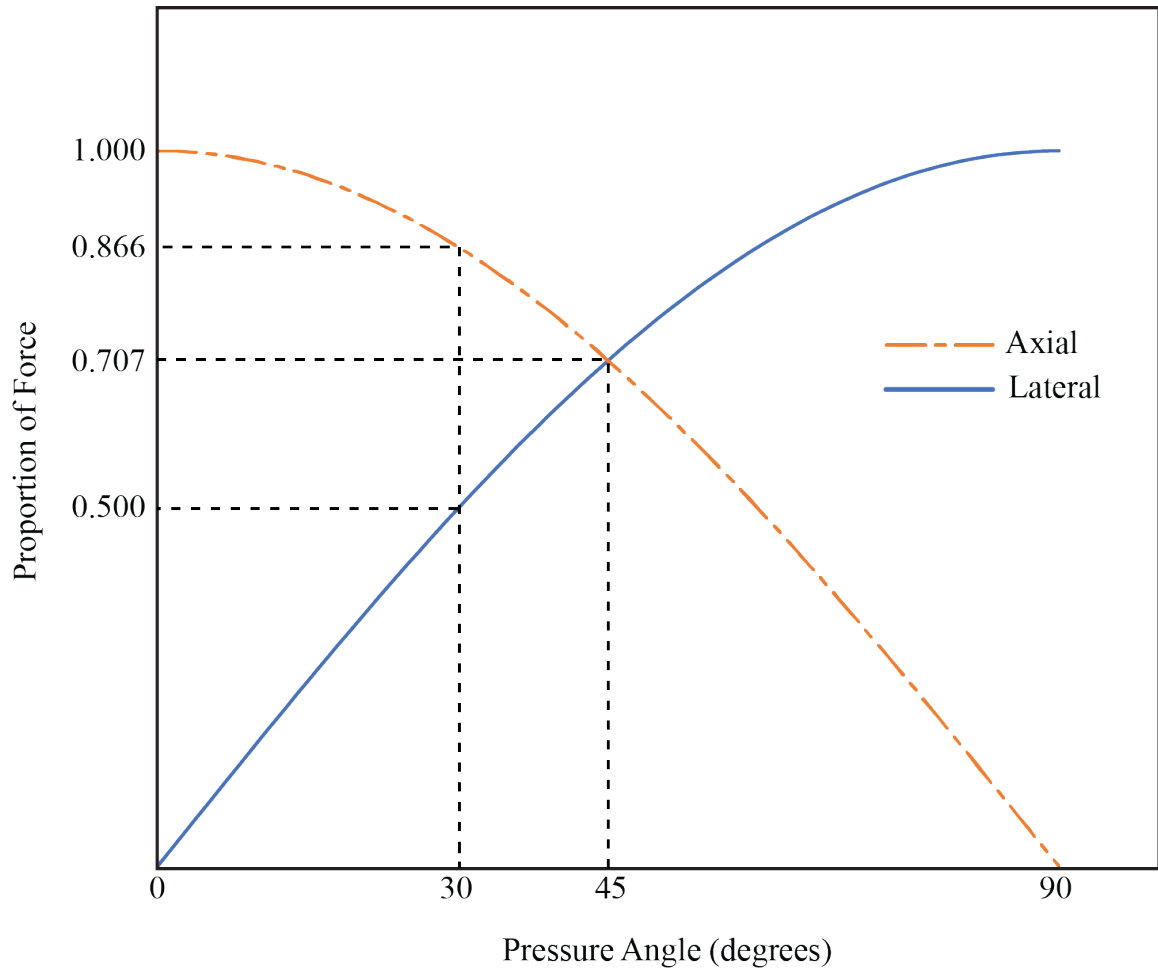


**Figure 3.4:** Axial and lateral components of applied force based on pressure angle

## 3.3 Dynamic Tests

### 3.3.1 Acrylic Cam Profile Testing

In order to efficiently produce the cam profiles for testing it was important to ensure that an acrylic cam would effectively reproduce the data that a steel cam would. The lateral forces measured during multiple trials with the steel and plastic profiles resulted in the data seen in Figure 3.5, which suggests that the acrylic cam profile is suitable for testing when forces are limited to 150N.

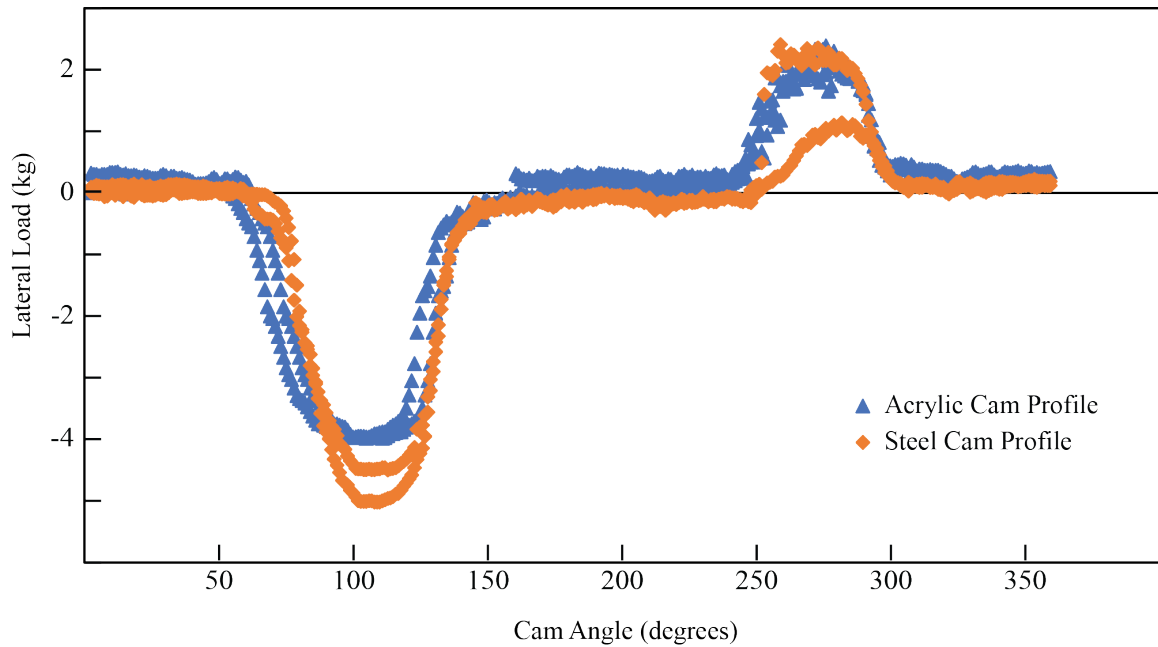


**Figure 3.5:** Comparison of lateral forces on steel and plastic cam profiles

This allows for the profiles to be easily machined either by CNC milling or laser cutting. The lateral force measurements also agree with the theoretical lateral forces based on the unequal lateral loading according to the previous results.

The profiles in Figure 3.6, represent the initial cam profiles that were tested consisting of polynomial 3-4-5 cam profiles which begin and end with pressure angles of 0 and reach a maximum of 20, 25, and 30 degrees.



**Figure 3.6:** Polynomial steel and acrylic cam profiles: 30, 30, 25, and 20 degrees from top left to bottom right)

### 3.3.2 Constant Pressure Angle Testing

In order to better understand the effects of the pressure angle limitation, testing was then performed using the constant pressure angle cams as seen in Figure 3.9. The 30, 35, and 40 degree constant pressure angle cams were then tested in order to better understand how the undesirable lateral force changes. The data seen in Figure 3.7 shows that the lateral force increases as the distance  $r$  increases, while the axial force and pressure angle are held constant. Once the follower reaches the dwell where the lateral force goes to 0 as the pressure angle is also 0. This same behaviour is mirrored on the fall but with a smaller lateral force which agrees with Equation (3.8). The curves for the 30 and 35 degree pressure angle tests agree with those for the 40 degree tests. while the offset in the curves is due to the stepper motor approaching its peak



torque and briefly slipping causing missed steps. As per the equations developed for the torque during the rise and fall, the lateral forces are expected to be larger during the rise portion and smaller during the fall, as the lateral force directly effects the torque.

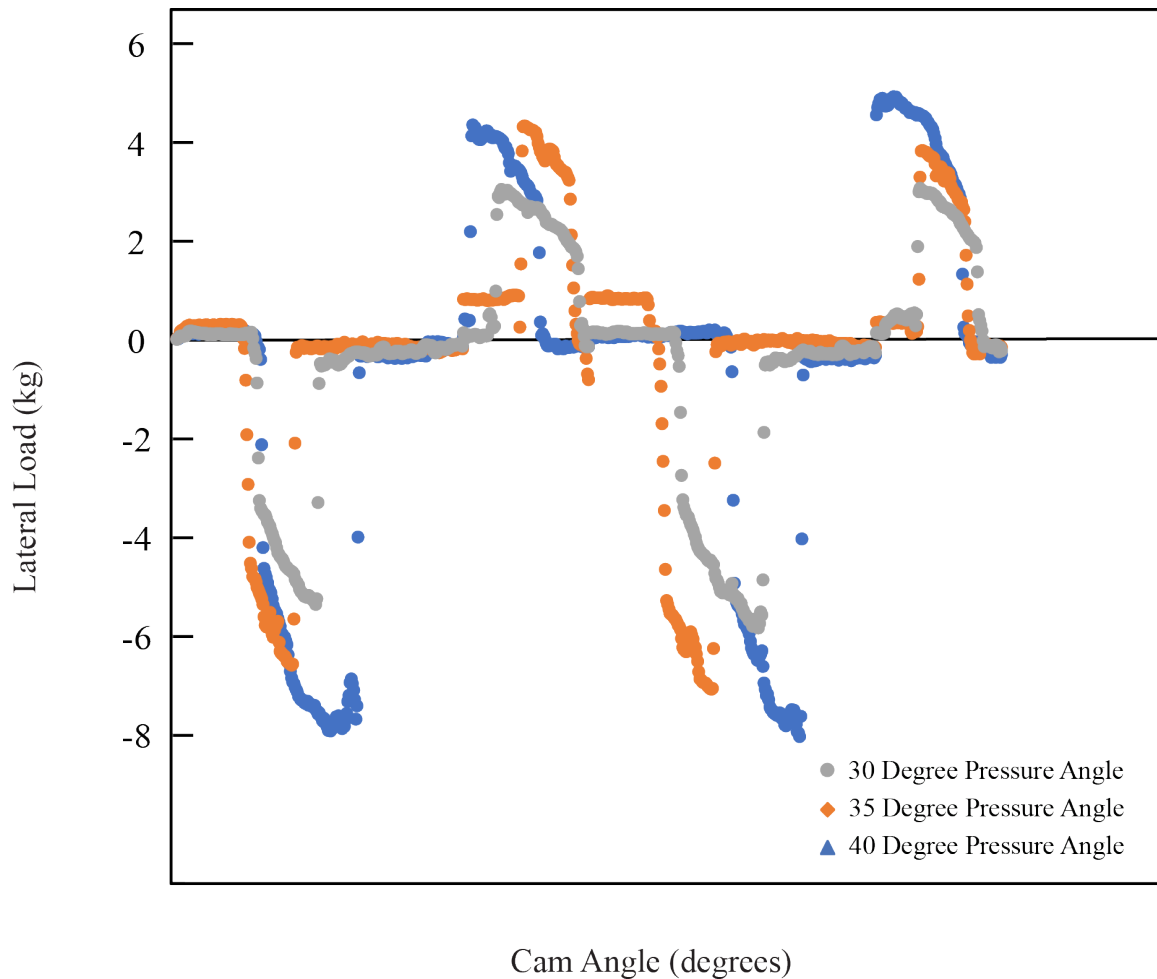


**Figure 3.7:** Lateral load produced by 30, 35 and 40 degree pressure angle cams

When the lateral forces are compared between the rise and fall, the forces decrease by 20-30% across the various pressure angle cams tested. Based on a maximum pressure angle ranging from 30-40 degrees, the difference between the lateral forces on the rise and fall should be as high as 36% for the 40 degree pressure angle cam and as high

as 14% for 30 degree pressure angle cam. With the additional  $\pm 4.9\%$  error from the test apparatus factored in, the recorded values are within reasonable limits. This suggests that the pressure angle limits can exceed 30 degrees if necessary but in order to minimize the input torque and optimize the potential of recovering energy from the system they should be reduced as much as possible.

## 3.4 Static Tests

### 3.4.1 Static Testing (no spring)

In order to better understand the potential pressure angle limits, the following cam profiles were developed using a fixed pressure angle in order to ensure that the pressure angle would not have to be approximated based on the measured distance  $r$ . As seen in Figure 3.8, four cam profiles were created with 20, 30, 35, and 40 degree pressure angles. This was achieved by back calculating the radius of the cam at known increments by inputting the desired pressure angle.



**Figure 3.8:** From top to bottom 20, 30, 35, and 40 degree constant pressure angle cam profiles

Unlike most cams where the pressure angle ranges from 0 to a maximum and back to 0, the constant pressure angle cam results in a fixed duration  $\beta$  since the pressure angle is constant throughout the entire duration.

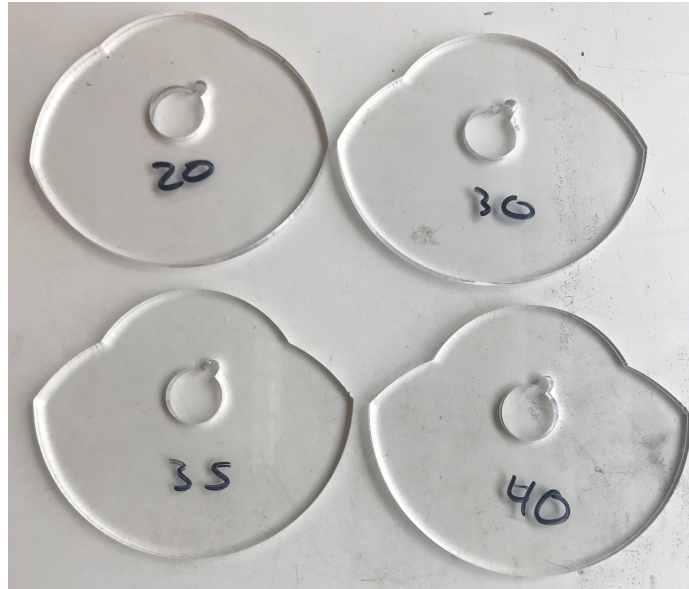


**Figure 3.9:** Constant pressure angle cam profiles

This results in the sharp points found at the beginning and end of the rise and fall portion of the cam profiles which can be seen in Figure 3.8 and Figure 3.9. This also explains why the pressure angle and displacement program chosen for a cam profile can have such a significant effect on the efficient operation.

Based on Equation (3.7), the torque that can be recovered from the system is a function of the pressure angle, length  $r$ , and applied force  $F_a$ . Using the static test apparatus the stop can be positioned at various locations in order to measure the torque based on an applied load while knowing the pressure angle and measured length  $r$ . From Figure 3.10 it can be seen that the available output torque increases with both the applied axial force  $F_a$  and increase in pressure angle  $\alpha$ . The results

from the analytical solutions agree with the experimental data when considering the error from the test apparatus. This suggests that the proposed model for recovering energy from the system is valid.

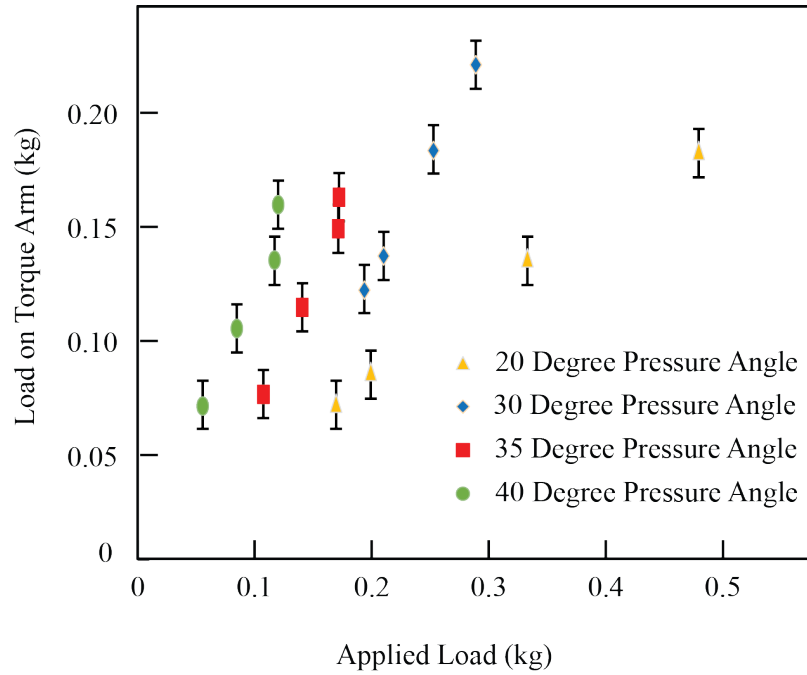


**Figure 3.10**

## 3.5 Conclusion

An analytical investigation was performed in attempts to better understand the potential of a cam follower system to recover energy during the fall portion of its cycle. Free body diagrams of the cam were created to help determine if and how the cam follower mechanism could recover energy from the system. An analytical model was proposed to understand how the output torque was related to the input torque. This was followed by the design and fabrication of two test apparatuses in order to perform dynamic and static testing. Lastly experiments were performed in order to validate the model and better understand whether the 30 degree pressure angle limit could be exceeded and what effects it would have on the recovery of energy from the system.

- It was shown that the input and output torque are effected differently by pressure angle and that energy can be recovered through a cam follower system.
- It was found that in order to recover the most amount of energy from the system, the pressure angle should be kept as small as possible.
- The model showed that peak output torque is achieved at a 45 degree pressure angle which results in only half of the potential energy extraction.
- The suggested maximum pressure angle limit of 30 degrees was exceed by 10 degrees with the only concern being additional lateral force development. Thus suitable design consideration should be taken when exceeding 30 degree pressure angles.

### 3.5.1 Recommendations

- Further investigate the potential energy recovery of constant pressure angle cam profiles with efficient transitions from dwell to fall and fall to dwell. Also investigating the effects these displacement profiles would have on the velocity, acceleration, and jerk profiles.
- Test the validity of these pressure angle claims with higher speeds in order to understand the rotational velocity limits.
- Determine whether or not the same principal of energy recovery can be applied to other cam and follower combinations and what the limits of those may be.

# Bibliography

- [1] Harold Rothbart. *Cams: Design Dynamics, and Accuracy*. Wiley, 1965.
- [2] J. E. Shigley and J. Uicker. *Theory of Machines and Mechanisms*. McGraw Hill, New York, 1980.
- [3] F. Y. Chen. *Mechanics and Design of Cam Mechanisms*. Pergamon Press, New York, 1982.
- [4] Fan Y. Chen. A survey of the state of the art of cam system dynamics. *Mechanism and Machine Theory*, 12(3):201–224, 1977.
- [5] Jos Maria Bezerra Silva, Flix Christian G Santos, and Jos Maria Andrade Barbosa. Obtaining the maximum pressure angle in translating radial cam-follower. *Journal of Mechanical Design*, 2011.
- [6] T. K. Naskar and S. Acharyya. Measuring camfollower performance. *Mechanism and Machine Theory*, 45(4):678–691, 2010.
- [7] Koomok M. R. and Muffley. *Plate cam Design Pressure Angle Analysis*. Wiley, New York, 1955.

- [8] B. L. MacCarthy and N. D. Burns. An evaluation of spline functions for use in cam design. *Proceedings of the Institution of Mechanical Engineers, Part C: Journal of Mechanical Engineering Science*, 199(3):239–248, 1985.
- [9] E. Sandgren and R. L. West. Shape optimization of cam profiles using a b-spline representation. *Journal of Mechanisms, Transmissions, and Automation in Design*, 111(2):195–201, 1989.
- [10] D. M. Tsay and Jr C. O. Huey. Application of rational b-splines to the synthesis of cam-follower motion programs. *Journal of Mechanical Design*, 115(3):621–626, 1993.
- [11] K. Yoon and S. S. Rao. Cam motion synthesis using cubic splines. *Journal of Mechanical Design*, 115(3):441–446, 1993.
- [12] Q. Yu and H. P. Lee. Size optimization of cam mechanisms with translating roller followers. *Proceedings of the Institution of Mechanical Engineers*, 212(5):381, 1998.
- [13] Hong-Sen Yan, Mi-Ching Tsai, and Meng-Hui Hsu. A variable-speed method for improving motion characteristics of cam-follower systems. *Journal of Mechanical Design*, 118(2):250–258, 1996.
- [14] H. S. Yan, M. C. Tsai, and M. H. Hsu. An experimental study of the effects of cam speeds on cam-follower systems. *Mechanism and Machine Theory*, 31(4):397–412, 1996.



- [15] Jr J. J. Uicker, J. Denavit, and R. S. Hartenberg. An iterative method for the displacement analysis of spatial mechanisms. *Journal of Applied Mechanics*, 31(2):309–314, 1964.
- [16] Robert L Norton. *Cam Design and Manufacturing Handbook*. Thomson Press, New York, 2 edition, 2009.
- [17] P. Flores. *Cam Size Optimization of Disc Cam-Follower Mechanisms with Translating Roller Followers*, pages 225–233. Springer Netherlands, Dordrecht, 2010.
- [18] Waldron. *Kinematics, Dynamics And Design Of Machinery, 2Nd Ed (With Cd)*. Wiley India Pvt. Limited, 2007.
- [19] M. P. Koster. Effect of flexibility of driving shaft on the dynamic behavior of a cam mechanism. *Journal of Engineering for Industry*, 97(2):595–602, 1975.
- [20] C. Lanni et al. Numerical and experimental analyses of radial cams with circular-arc profiles. *Proceedings of the Institution of Mechanical Engineers*, vol. 220:111–125, 2006.
- [21] S. Carra, R. Garziera, and M. Pellegrini. Synthesis of cams with negative radius follower and evaluation of the pressure angle. *Mechanism and Machine Theory*, 39(10):1017–1032, 2004.
- [22] Forrest W. Flocker. Addressing cam wear and follower jump in single-dwell cam-follower systems with an adjustable modified trapezoidal acceleration cam profile. *Journal of Engineering for Gas Turbines and Power*, 131(3):032804–032804–8, 2009.

- [23] Ramiro H. Bravo and Forrest W. Flocker. Optimizing cam profiles using the particle swarm technique. *Journal of Mechanical Design*, 133(9):091003–091003–11, 2011.
- [24] Zhiming Ji and Yazan A Manna. Size minimization of disc cams with roller-followers under pressure angle constraint. *Proceedings of the Institution of Mechanical Engineers, Part C: Journal of Mechanical Engineering Science*, 222(12):2475–2484, 2008.
- [25] D. H. Kim and T. C. Tsao. Robust performance control of electrohydraulic actuators for electronic cam motion generation. *IEEE Transactions on Control Systems Technology*, 8(2):220–227, 2000.
- [26] Der Min Tsay and Hsien Min Wei. A general approach to the determination of planar and spatial cam profiles. *Journal of Mechanical Design*, 118(2):259–265, 1996.
- [27] Hong-Sen Yan and Wei-Ren Chen. On the output motion characteristics of variable input speed servo-controlled slider-crank mechanisms. *Mechanism and Machine Theory*, 35(4):541–561, 2000.
- [28] Hong-Sen Yan and Wei-Ren Chen. A variable input speed approach for improving the output motion characteristics of watt-type presses. *International Journal of Machine Tools and Manufacture*, 40(5):675–690, 2000.
- [29] Yan-an Yao, Ce Zhang, and Hong-Sen Yan. Motion control of cam mechanisms. *Mechanism and Machine Theory*, 35(4):593–607, 2000.